Syntheses of Mono and Bimetallic Cyamelurate Polymers with Reversible Chromic Behaviour

Midhun Mohan,[a] Sanil Rajak,[a] Alexandre A. Tremblay,[a] Thierry Maris[b] and Adam Duong*[,a]

[a] *Département de Chimie, Biochimie et physique* and *Institut de Recherche sur l'Hydrogène,* Université du Québec à Trois-Rivières, Trois-Rivières, Québec, G9A 5H7, Canada
[b] *Département de Chimie,* Université de Montréal, Montréal, Québec, H3C 3J7, Canada

*To whom correspondence should be addressed. E-mail : adam.duong@uqtr.ca

Contents

Experimental Section

General notes. Potassium cyamelurate K_3L was synthesized by known reported methods. All chemicals and solvents were purchased from commercial sources and were used without further purification.

General procedure for preparing MOPs-(1-4). Aqueous solutions of 0.1 mmol of potassium cyamelurate (6 mL) and 0.6 mmol of metal salt ($MnSO_4$, $Co(NO_3)_2.6H_2O$, $Ni(NO_3)_2.6H_2O$ or $Zn(NO_3)_2.6H_2O$) (6 mL) were mixed together at room temperature. The mixture was stirred for 2 h and then kept at room temperature for 12 h. Crystalline samples of MOPs-(**1-4**) were collected by filtration.

MOP-1. Amber crystal, yield 91 %. IR(ATR) 3546, 3348, 3240, 2970, 2797, 1678, 1637, 1454, 1439, 1401, 1369, 1331, 1316, 1198, 1148, 1124, 978, 963, 832, 798, 760 cm^{-1}. Anal. Calcd for $Mn_2(C_6N_7O_3H)_2.10H_2O$: C, 19.71; H, 2.95; N, 26.28. Found: C, 19.74; H, 3.31, N, 26.85.

MOP-2. Pink crystal, yield 82 %. IR(ATR) 3566, 3462, 3190, 2946, 2797, 1681, 1621, 1487, 1439, 1401, 1369, 1331, 1313, 1204, 1148, 1129, 978, 963, 832, 798, 957, 707, 692 cm^{-1}. Anal. Calcd for $Co_2(C_6N_7O_3H)_2.10H_2O$: C, 19.53; H, 2.97; N, 26.03. Found: C, 19.52; H, 3.28; N, 26.56.

MOP-3. Cyan crystal, yield 80 %. IR(ATR) 3573, 3472, 3198, 2946, 2797, 1681, 1487, 1436, 1403, 1369, 1331, 1315, 1205, 1169, 1148, 1124, 978, 965, 832, 799, 789, 757, 710, 695 cm^{-1}. Anal. Calcd for $Ni_2(C_6N_7O_3H)_2.10H_2O$: C, 19.22; H, 2.79; N, 25.76. Found: C, 19.12; H, 3.21; N, 26.01.

MOP-4. Colourless crystal, yield 80 % based on metal salt. IR(ATR) 3390, 3147, 2958, 2797, 1681, 1597, 1516, 1487, 1455, 1403, 1369, 1329, 1315, 1201, 1194, 1161, 1148, 1124, 978, 965,849, 832, 799, 762, 716, 692 cm^{-1}; Anal. Calcd for $Zn_2(C_6N_7O_3H)_2.10H_2O$: C, 20.28; H, 2.66; N, 25.26. Found: C, 19.24, H 2.96, N 26.17.

General procedure for preparing MMOPs-(5-7). Aqueous solutions of 0.1 mmol of potassium cyamelurate (6 mL) and 0.3 mmol equimolar ratio of the two metals salts (A/B =

$Mn(SO_4)/Co(NO_3)_2$. $6H_2O$, $Mn(SO_4)/Ni(NO_3)_2.6H_2O$, or $Ni(NO_3)_2.6H_2O/Zn(NO_3)_2.6H_2O$) (6 mL) were mixed together at room temperature. The mixture was stirred for 2 h and then kept at room temperature for 12 h. Crystalline samples of MMOPs-(**5-7**) were collected by filtration.

MMOP-5. Pink crystal, yield 89 %. IR(ATR) 3567, 3459, 3216, 2964, 2749, 1699, 1682, 1634, 1488, 1455, 1435, 1404, 1369, 1331, 1315, 1201, 1161, 1148, 1125, 1125, 977, 964, 832, 799, 788, 761, 709, 691 cm^{-1}. Anal. Calcd for $Mn_{0.26}Co_{1.74}(C_6N_7O_3H)_2.10H_2O$: C, 19.83; H, 3.11; N, 26.32. Found: C, 19.68; H, 3.03, N, 26.78.

MMOP-6. Cyan crystal, yield 90 %. IR(ATR) 3565, 3462, 3207, 2958, 2793, 1682, 1635, 1489, 1454, 1438, 1403, 1369, 1329, 1316, 1202, 1163, 1148, 1126, 978, 964, 833, 799, 787, 760, 709, 693 cm^{-1}. Anal. Calcd for $Mn_{0.32}Ni_{1.68}(C_6N_7O_3H)_2.10H_2O$: C, 19.64; H, 2.99; N, 26.52. Found: C, 19.69; H, 3.03, N, 26.79.

MMOP-7. Cyan crystal, yield 80 %. IR(ATR) 3564, 3463, 3192, 2934, 2790, 1682, 1633, 1489, 1455, 1438, 1402, 1368, 1330, 1315, 1204, 1163, 1148, 1126, 979, 966, 833, 800, 788, 767, 759, 708, 694 cm^{-1}. Anal. Calcd for $Ni_{1.41}Zn_{0.59}(C_6N_7O_3H)_2.10H_2O$: C, 19.43; H, 2.96; N, 26.06. Found: C, 19.41; H, 2.99, N, 26.41.

Studies of Single-Crystal Structures of Metal-Organic Polymers (1-4) and Mixed Metal-Organic Polymers (5-7)

The position of hydrogen atoms in the structures of MOPs-(**1-4**) are fully refined and determined using the difference Fourier map. For MOP-**1**, MOP-**2** and MOP-**4**, the first 11 Q peaks with electron density maxima appearing in the map correspond exactly to the position of the 11 hydrogen atoms in the asymmetric unit. For MOP-**3**, due to residual electron density around the Ni atom from absorption the Q peaks of all hydrogen atoms are not all in the first 11. For each difference Fourier map of MOPs-(**1-4**), notice that one of the Q peak is closer to the nitrogen atom of the heptazine confirming the presence of N-H group in the structures.

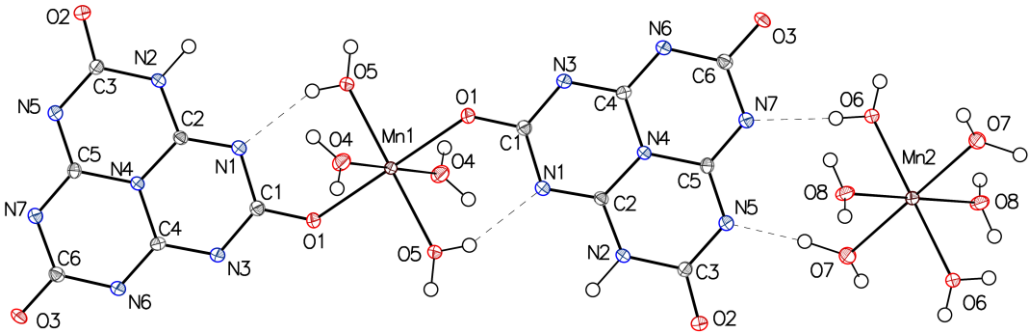

Figure S1. Thermal atomic displacement ellipsoid plot of MOP-**1**. The ellipsoids of non-hydrogen atoms are drawn at 50% probability level, hydrogen atoms are represented by a sphere of arbitrary size, and hydrogen bonds are represented by dotted lines.

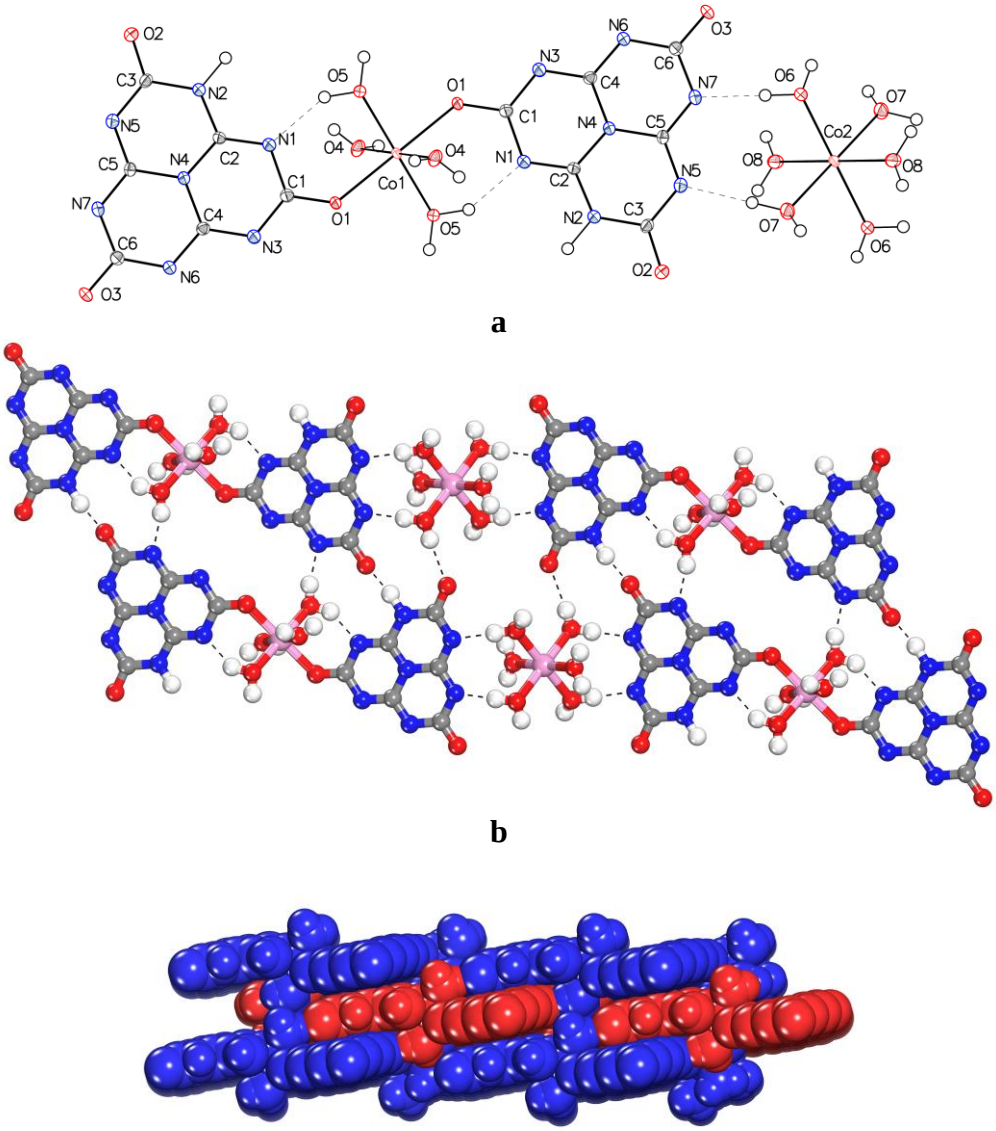

a

b

c

Figure S2. Crystal structure of MOP-**2**. a) Thermal atomic displacement ellipsoid plot of MOP-**2**. The ellipsoids of non-hydrogen atoms are drawn at 50% probability level, hydrogen atoms are represented by a sphere of arbitrary size, and hydrogen bonds are represented by dotted lines. b) View of the 2D sheets connected by coordination bonds and hydrogen bonds. Hydrogen bonds are represented in dotted lines, and cobalt atoms are shown in pink, carbon atoms in grey, hydrogen atoms in white, nitrogen atoms in blue, and oxygen atoms in red. c) Packing of the 2D sheets to form the three-dimensional structure. For more clarity layers marked in red and blue.

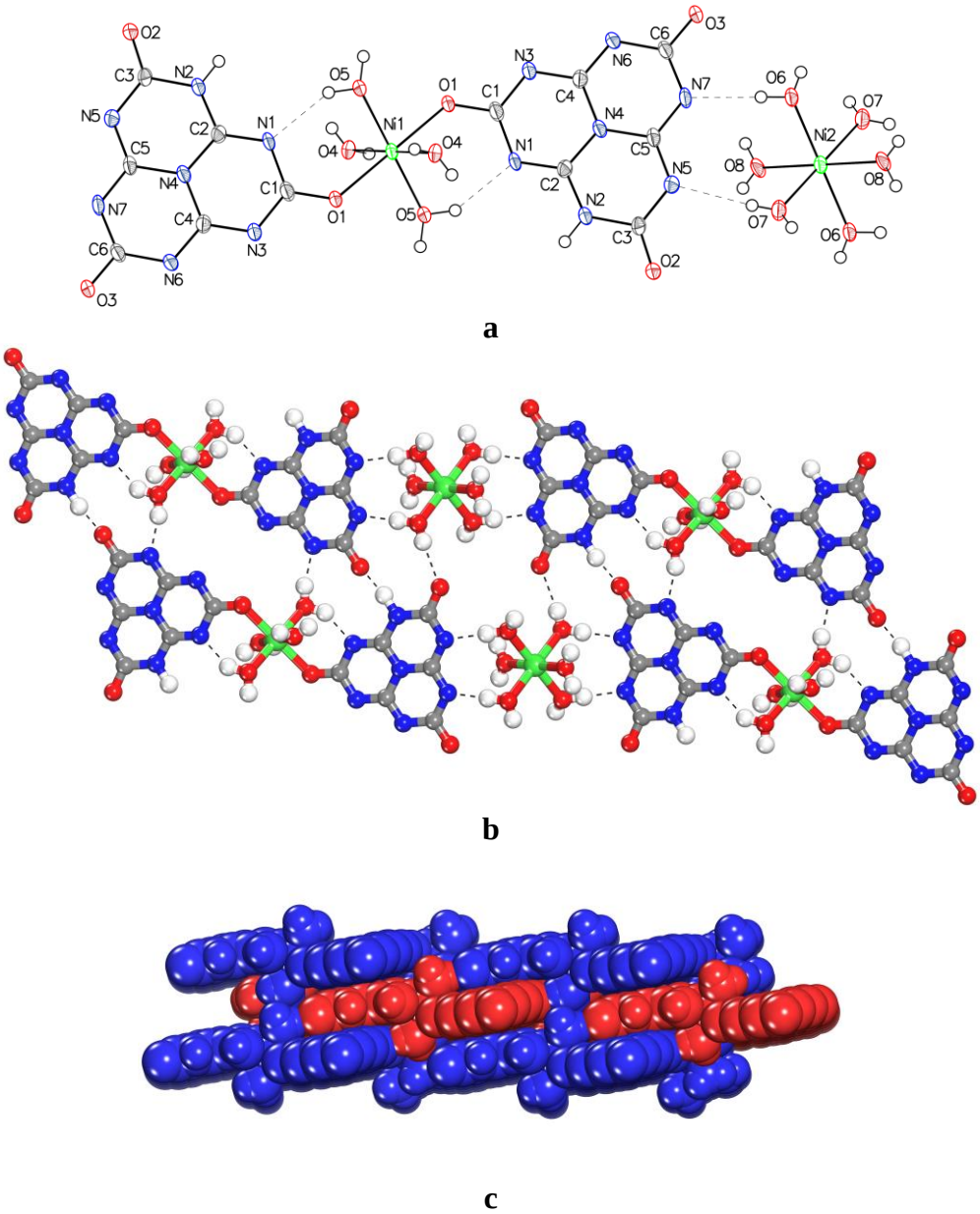

a

b

c

Figure S3. Crystal structure of MOP-**3**. a) Thermal atomic displacement ellipsoid plot of MOP-**3**. The ellipsoids of non-hydrogen atoms are drawn at 50% probability level, hydrogen atoms are represented by a sphere of arbitrary size, and hydrogen bonds are represented by dotted lines. b) View of the 2D sheets connected by coordination bonds and hydrogen bonds. Hydrogen bonds are represented in dotted lines, and nickel atoms are shown in green, carbon atoms in grey, hydrogen atoms in white, nitrogen atoms in blue, and oxygen atoms in red. c) Packing of the 2D sheets to form the three-dimensional structure. For more clarity layers marked in red and blue.

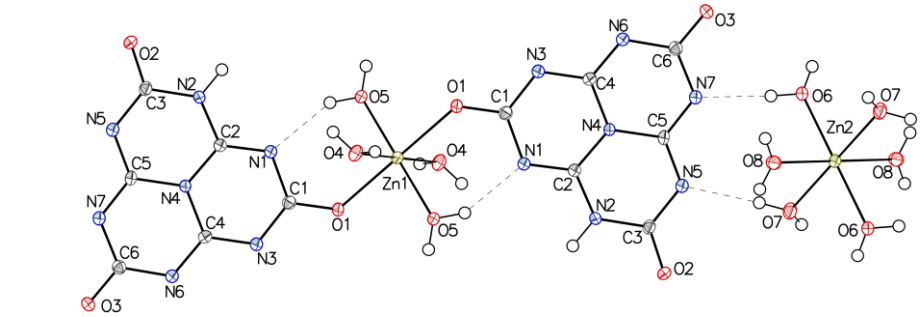

a

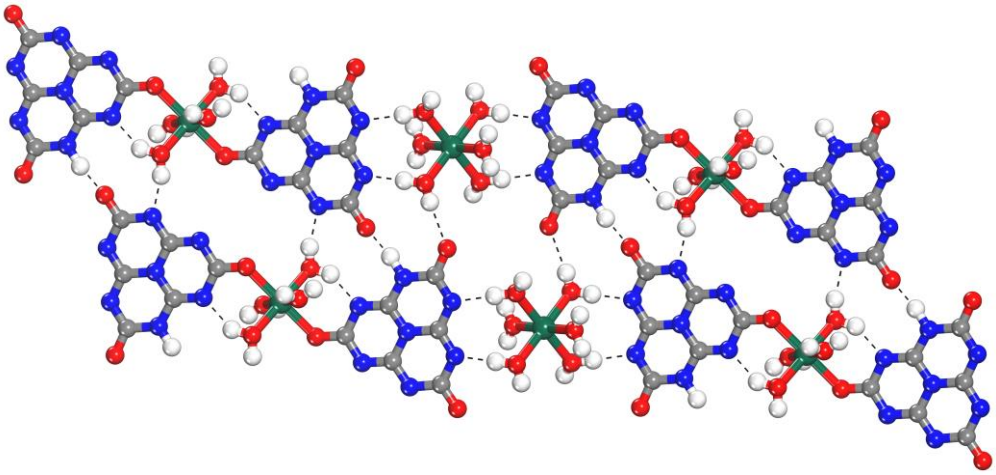

b

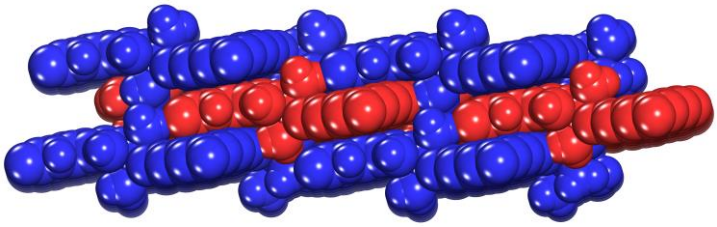

c

Figure S4. Crystal structure of MOP-**4**. a) Thermal atomic displacement ellipsoid plot of MOP-**4**. The ellipsoids of non-hydrogen atoms are drawn at 50% probability level, hydrogen atoms are represented by a sphere of arbitrary size, and hydrogen bonds are represented by dotted lines. b) View of the 2D sheets connected by coordination bonds and hydrogen bonds. Hydrogen bonds are represented in dotted lines, and zinc atoms are shown in olive-drab, carbon atoms in grey, hydrogen atoms in white, nitrogen atoms in blue, and oxygen atoms in red. c) Packing of the 2D sheets to form the three-dimensional structure. For more clarity layers marked in red and blue.

Table S1. Crystallographic Data of Metal-Organic Polymers (**1-4**).

	MOP-1	**MOP-2**	**MOP-3**	**MOP-4**
Formula	$Mn_2C_{12}H_{22}N_{14}O_{16}$	$Co_2C_{12}H_{22}N_{14}O_{16}$	$Ni_2C_{12}H_{22}N_{14}O_{16}$	$Zn_2C_{12}H_{22}N_{14}O_{16}$
Crystal System	Triclinic	Triclinic	Triclinic	Triclinic
Mr	728.31	736.29	735.82	749.17
T (K)	100	120	100	100
Radiation	GaKα	GaKα	GaKα	GaKα
λ (Å)	1.34139	1.34139	1.34139	1.34139
F (000)	370	374	376	380
Space group	$P\bar{1}$	$P\bar{1}$	$P\bar{1}$	$P\bar{1}$
a (Å)	6.9844(4)	7.3633(3)	7.3698(3)	7.4188(3)
b (Å)	8.7175(5)	8.6464(3)	8.6190(3)	8.6369(4)
c (Å)	10.0198(6)	9.2763(3)	9.1796(3)	9.2126(4)
α (deg)	79.079(2)	77.947(2)	78.027(2)	77.798(2)
β (deg)	81.581(2)	84.247(2)	84.389(2)	84.443(2)
γ (deg)	84.507(2)	87.228(2)	86.957(2)	87.127(2)
V ($Å^3$)	591.11(6)	574.43(4)	567.36(4)	573.99(4)
Z	1	1	1	1
ρ_{calcd} (g cm^{-3})	2.046	2.128	2.154	2.167
μ (mm^{-1})	6.655	8.627	9.766	2.388
No. measured reflections	32337	30851	18351	23186
No. independent reflections	2698	2633	2490	2636
No. obsd. reflections I>2σ(I)	2632	2457	2599	2454
Nb Params	246	246	246	246
R_1, I>2σ (%)	0.0215	0.0287	0.0742	0.0264
R_1, all data (%)	0.0219	0.0307	0.1017	0.0284
ωR_2, I>2σ(I) (%)	0.0633	0.0764	0.1723	0.0705
ωR_2, all data (%)	0.0639	0.0783	0.1909	0.0719
GoF	1.116	1.093	1.101	1.067

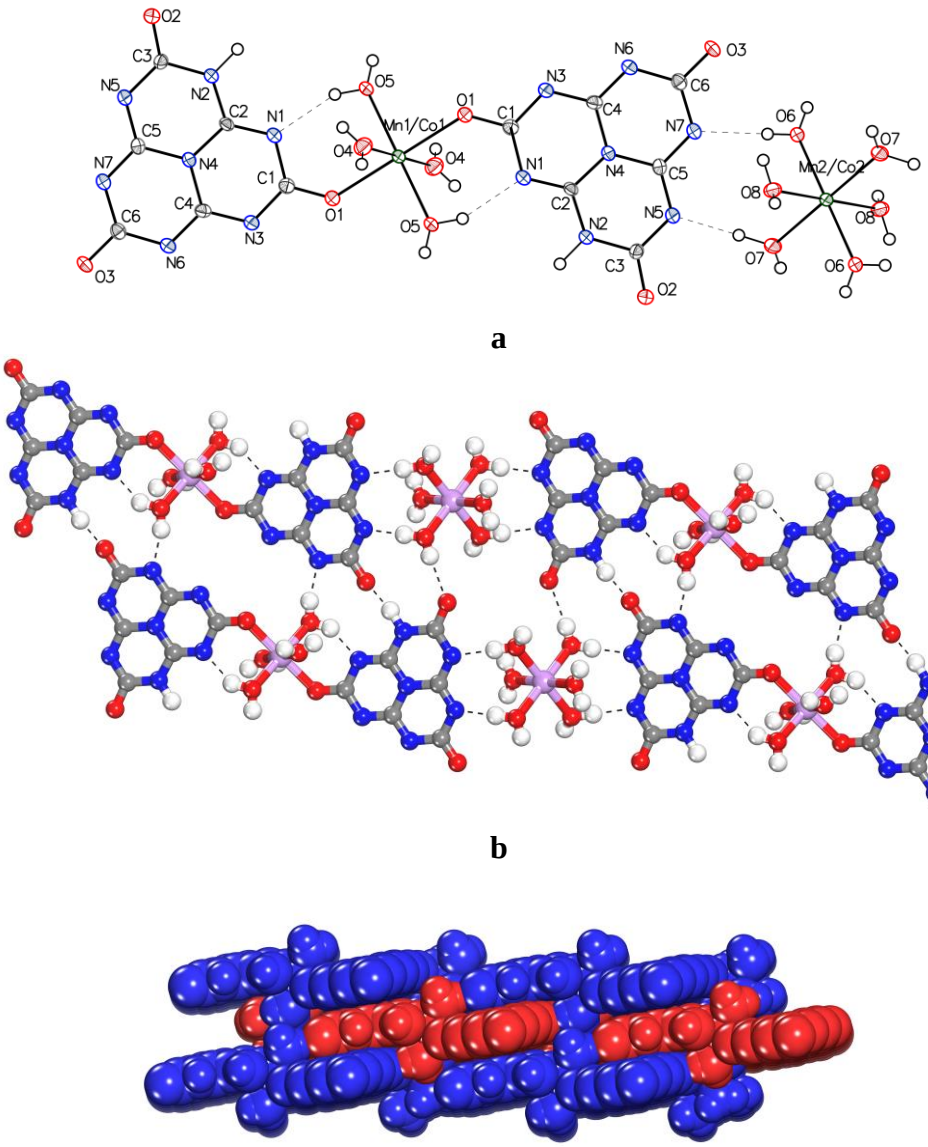

Figure S5. Crystal structure of MMOP-**5**. a) Thermal atomic displacement ellipsoid plot of MMOP-**5**. The ellipsoids of non-hydrogen atoms are drawn at 50% probability level, hydrogen atoms are represented by a sphere of arbitrary size, and hydrogen bonds are represented by dotted lines. b) View of the 2D sheets connected by coordination bonds and hydrogen bonds. Hydrogen bonds are represented in dotted lines, and manganese and cobalt atoms are shown in dark green, carbon atoms in grey, hydrogen atoms in white, nitrogen atoms in blue, and oxygen atoms in red. c) Packing of the 2D sheets to form the three-dimensional structure. For more clarity layers marked in red and blue.

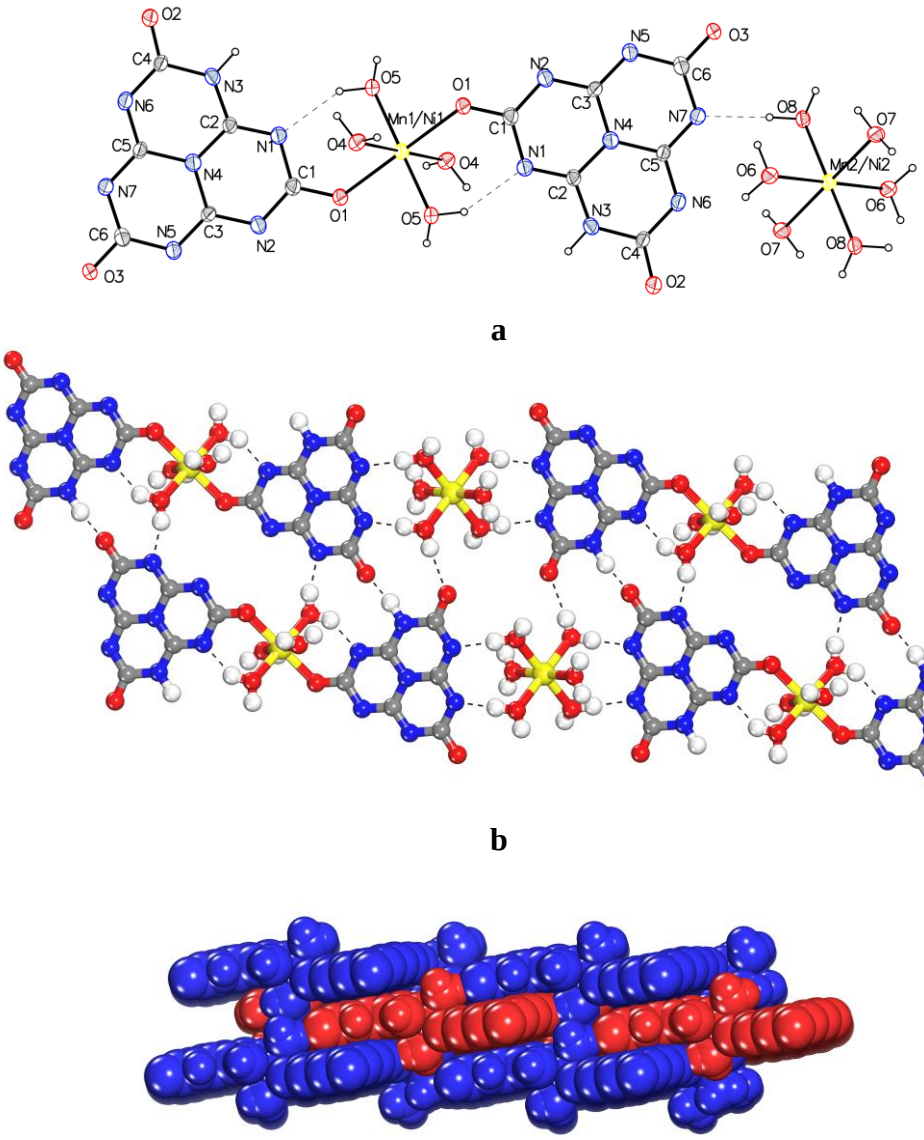

Figure S6. Crystal structure of MMOP-**6**. a) Thermal atomic displacement ellipsoid plot of MMOP-**6**. The ellipsoids of non-hydrogen atoms are drawn at 50% probability level, hydrogen atoms are represented by a sphere of arbitrary size, and hydrogen bonds are represented by dotted lines. b) View of the 2D sheets connected by coordination bonds and hydrogen bonds. Hydrogen bonds are represented in dotted lines, and manganese and nickel atoms are shown in yellow, carbon atoms in grey, hydrogen atoms in white, nitrogen atoms in blue, and oxygen atoms in red. c) Packing of the 2D sheets to form the three-dimensional structure. For more clarity layers marked in red and blue.

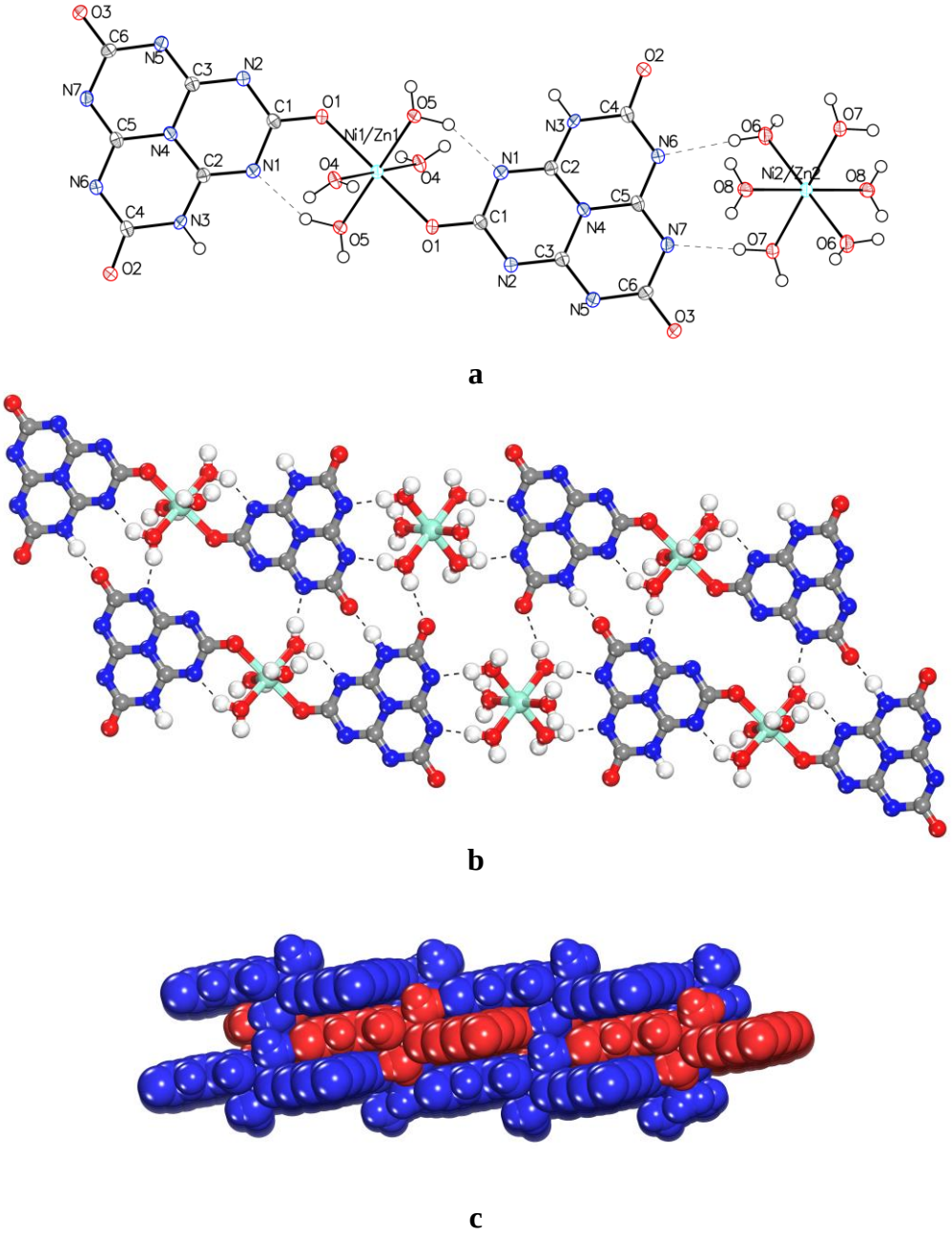

a

b

c

Figure S7. Crystal structure of MMOP-**7**. a) Thermal atomic displacement ellipsoid plot of MMOP-**7**. The ellipsoids of non-hydrogen atoms are drawn at 50% probability level, hydrogen atoms are represented by a sphere of arbitrary size, and hydrogen bonds are represented by dotted lines. b) View of the 2D sheets connected by coordination bonds and hydrogen bonds. Hydrogen bonds are represented in dotted lines, and nickel and zinc atoms are shown in light blue, carbon atoms in grey, hydrogen atoms in white, nitrogen atoms in blue, and oxygen atoms in red. c) Packing of the 2D sheets to form the three-dimensional structure. For more clarity layers marked in red and blue.

Table S2. Crystallographic Data of Mixed Metal-Organic Polymers (**5-7**).

	MMOP-5	**MMOP-6**	**MMOP-7**
Formula	$Mn_{0.3}Co_{1.7}C_{12}H_{22}N_{14}O_{16}$	$Mn_{0.84}Ni_{1.16}C_{12}H_{22}N_{14}O_{16}$	$Ni_{1.41}Zn_{0.59}C_{12}H_{22}N_{14}O_{16}$
Crystal System	Triclinic	Triclinic	Triclinic
Mr	735.10	732.69	739.78
T (K)	120	100	100
Radiation	GaKα	GaKα	GaKα
λ (Å)	1.34139	1.34139	1.34139
F (000)	373	373	377
Space group	$P\bar{1}$	$P\bar{1}$	$P\bar{1}$
a (Å)	6.999(2)	7.2816(16)	7.3891(3)
b (Å)	8.6955(2)	8.6497(19)	8.6307(3)
c (Å)	9.8777(3)	9.4431(19)	9.1887(4)
α (deg)	78.7700(10)	78.648(13)	77.928(2)
β (deg)	81.6070(10)	83.519(13)	84.470(2)
γ (deg)	85.0940(10)	87.455(14)	87.086(2)
V ($Å^3$)	582.39(3)	579.2(2)	570.08(4)
Z	1	1	1
ρ_{calcd} (g cm^{-3})	2.096	2.100	2.155
μ (mm^{-1})	8.245	8.405	7.566
No. measured reflections	27640	6859	16725
No. independent reflections	2658	2018	2583
No. obsd. reflections I>2σ(I)	2678	2208	2613
Nb Params	247	209	248
R_1, I>2σ (%)	0.0508	0.1045	0.0499
R_1, all data (%)	0.0586	0.1325	0.0572
ωR_2, I>2σ(I) (%)	0.0962	0.2826	0.1096
ωR_2, all data (%)	0.0988	0.3137	0.1148
GoF	1.217	1.071	1.158

Table S3. Hydrogen bond geometry (Å, ˚) of MOP-**1**.

D*—H···*A	***D*—H**	**H···*A***	***D*···*A***	***D*—H···*A***
O4—H4b···O2i	0.84 (3)	1.86 (3)	2.6845 (15)	170 (3)
O5—H5a···N6ii	0.82 (3)	1.97 (3)	2.7717 (16)	166 (3)
O5—H5b···N1	0.79 (3)	2.04 (3)	2.7709 (16)	154 (3)
O6—H6a···O2iii	0.80 (3)	2.12 (3)	2.8919 (15)	163 (2)
O6—H6b···N7	0.79 (3)	1.96 (3)	2.7554 (16)	177 (3)
O7—H7a···N5	0.99 (3)	1.77 (3)	2.7533 (16)	170 (2)
O8—H8b···N3iv	0.85 (3)	1.86 (3)	2.7055 (15)	176 (2)
N2—H2···O3ii	1.00 (2)	1.73 (2)	2.7243 (14)	176.7 (19)

Symmetry codes: (i) *x*−1, *y*, *z*+1; (ii) *x*, *y*+1, *z*; (iii) *x*, *y*−1, *z*; (iv) *x*+1, *y*, *z*−1.

Table S4. Hydrogen bond geometry (Å, ˚) of MOP-**2**.

D*—H···*A	***D*—H**	**H···*A***	***D*···*A***	***D*—H···*A***
O4—H4*A*···O2^{i}	0.79 (3)	1.94 (3)	2.7180 (18)	167 (3)
O4—H4*B*···O2^{ii}	0.92 (4)	2.07 (4)	2.9800 (19)	170 (3)
O5—H5*A*···O3^{iii}	0.92 (3)	2.51 (3)	2.9905 (18)	113 (2)
O5—H5*A*···N1	0.92 (3)	1.89 (3)	2.716 (2)	148 (3)
O5—H5*B*···N6^{iii}	0.90 (3)	1.80 (3)	2.682 (2)	167 (3)
O6—H6*A*···O2^{iv}	0.82 (3)	2.12 (3)	2.9220 (19)	166 (3)
O6—H6*B*···N7	0.92 (3)	1.81 (3)	2.730 (2)	178 (3)
O7—H7*A*···N5	0.93 (3)	1.92 (3)	2.835 (2)	171 (2)
O7—H7*B*···O1^{v}	0.94 (3)	2.00 (4)	2.8868 (18)	157 (3)
O8—H8*A*···N3^{v}	0.85 (3)	1.95 (3)	2.785 (2)	168 (3)
O8—H8*B*···O1^{vi}	0.90 (4)	2.55 (4)	3.0698 (18)	117 (3)
O8—H8*B*···O4^{vii}	0.90 (4)	2.19 (4)	3.0311 (19)	155 (3)
O8—H8*B*···O5^{vii}	0.90 (4)	2.63 (4)	3.3098 (19)	133 (3)
N2—H2···O3^{iii}	1.07 (3)	1.66 (3)	2.7200 (18)	171 (2)

Symmetry codes: (i) x+1, y, z−1; (ii) *−x+1, −y, −z+1*; (iii) x, y−1, z; (iv) x, y+1, z; (v) x−1, y, z+1; (vi) *−x, −y+1, −z+1*; (vii) x−1, y+1, z+1.

Table S5. Hydrogen bond geometry (Å, ˚) of MOP-**3**.

D*—H···*A	***D*—H**	**H···*A***	***D*···*A***	***D*—H···*A***
O4—H4*A*···O2^{i}	0.97 (8)	2.00 (8)	2.965 (7)	177 (7)
O4—H4*B*···O2^{ii}	0.71 (10)	2.08 (10)	2.719 (6)	151 (11)
O5—H5*A*···N6^{iii}	0.85 (7)	1.85 (8)	2.687 (7)	166 (6)
O5—H5*B*···O3^{iii}	0.81 (8)	2.54 (8)	2.982 (6)	116 (6)
O5—H5*B*···N1	0.81 (8)	1.99 (8)	2.707 (7)	148 (7)
N2—H2···O3^{iii}	0.84 (8)	1.88 (8)	2.714 (7)	170 (8)
O6—H6*A*···O2^{iv}	0.75 (9)	2.23 (9)	2.957 (7)	163 (9)
O6—H6*B*···N7	0.80 (9)	1.94 (9)	2.736 (6)	170 (8)
O7—H7*A*···O1^{v}	0.84 (9)	2.08 (10)	2.895 (6)	161 (8)
O7—H7*B*···N5	0.71 (8)	2.13 (8)	2.837 (7)	175 (8)

Symmetry codes: (i) x, y, z−1; (ii) −x+1, −y, −z+1; (iii) x, y−1, z; (iv) x, y+1, z; (v) x−1, y, z+1.

Table S6. Hydrogen bond geometry (Å, ˚) of MOP-**4**.

D*—H···*A	***D*—H**	**H···*A***	***D*···*A***	***D*—H···*A***
O4—H4*A*···O2^{i}	0.79 (2)	1.97 (2)	2.7198 (14)	158 (3)
O4—H4*B*···O2^{ii}	0.81 (2)	2.17 (2)	2.9835 (15)	175 (2)
O5—H5*A*···N6^{iii}	0.81 (2)	1.90 (2)	2.6828 (15)	164 (3)
O5—H5*B*···O3^{iii}	0.81 (2)	2.57 (2)	2.9903 (14)	114 (2)
O5—H5*B*···N1	0.81 (2)	1.98 (2)	2.7173 (15)	151 (2)
N2—H2···O3^{iii}	0.91 (2)	1.82 (2)	2.7176 (14)	171 (2)
O6—H6*A*···O2^{iv}	0.78 (1)	2.17 (2)	2.9303 (14)	164 (2)
O6—H6*B*···N7	0.80 (2)	1.94 (2)	2.7346 (15)	176 (2)
O7—H7*A*···N5	0.81 (1)	2.04 (1)	2.8367 (15)	172 (2)
O7—H7*B*···O1^{v}	0.81 (2)	2.15 (2)	2.8920 (14)	153 (3)
O8—H8*A*···N3^{v}	0.78 (1)	2.01 (2)	2.7839 (15)	175 (2)
O8—H8*B*···O1^{vi}	0.79 (2)	2.60 (2)	3.0714 (15)	120 (2)
O8—H8*B*···O4^{vii}	0.79 (2)	2.28 (2)	3.0240 (15)	158 (2)

Symmetry codes: (i) x−1, y, z+1; (ii) −x+1, −y+2, −z+1; (iii) x, y+1, z; (iv) x, y−1, z; (v) x+1, y, z−1; (vi) −x+2, −y+1, −z+1; (vii) x+1, y−1, z−1.

Table S7. Hydrogen bond geometry (Å, ˚) of MMOP-**5**.

D*—H···*A	***D*—H**	**H···*A***	***D*···*A***	***D*—H···*A***
O4—H4*A*···O7^{i}	0.75 (6)	2.31 (6)	3.008 (4)	154 (6)
O4—H4*B*···O2^{ii}	0.76 (5)	1.93 (5)	2.679 (4)	174 (5)
O5—H5*A*···N6^{iii}	0.78 (5)	2.01 (5)	2.760 (4)	162 (5)
O5—H5*B*···N1	0.85 (5)	1.95 (5)	2.750 (4)	157 (4)
N2—H2···O3^{iii}	0.99 (3)	1.72 (4)	2.716 (3)	178 (3)
O6—H6*A*···O2^{iv}	0.78 (5)	2.13 (5)	2.892 (3)	165 (4)
O6—H6*B*···N7	0.80 (5)	1.95 (5)	2.746 (4)	177 (5)
O7—H7*A*···N5	0.96 (5)	1.84 (5)	2.784 (4)	170 (4)
O7—H7*B*···O1^{v}	0.78 (5)	2.24 (5)	2.991 (3)	163 (4)
O8—H8*A*···O1^{vi}	0.75 (5)	2.21 (5)	2.940 (4)	165 (5)
O8—H8*B*···N3^{vii}	0.86 (5)	1.85 (5)	2.715 (4)	176 (4)

Symmetry codes: (i) −x+1, −y+2, −z+1; (ii) x−1, y, z+1; (iii) x, y+1, z; (iv) x, y−1, z; (v) x+1, y, z−1; (vi) x, y, z−1; (vii) −x+1, −y+1, −z+1.

Table S8. Hydrogen bond geometry (Å, ˚) of MMOP-**6**.

D*—H···*A	***D*—H**	**H···*A***	***D*···*A***	***D*—H···*A***
N3—H3···O3^{i}	0.88	1.85	2.725 (10)	171
O4—H4*A*···O2^{ii}	0.87	1.91	2.695 (11)	150
O4—H4*B*···O2^{iii}	0.87	2.25	3.106 (12)	169
O5—H5*A*···N5^{iv}	0.87	2.05	2.709 (11)	132
O5—H5*B*···N1^{v}	0.87	1.97	2.740 (11)	147
O5—H5*B*···O3^{iv}	0.87	2.62	3.077 (9)	114
O6—H6*A*···O4^{iii}	0.86	2.33	3.037 (11)	140
O6—H6*B*···N2^{vi}	0.86	1.99	2.766 (12)	150
O7—H7*A*···N5^{vii}	0.87	2.66	3.458 (12)	152
O7—H7*B*···O1^{vi}	0.87	2.06	2.932 (11)	177
O8—H8*A*···O2^{viii}	0.88	2.12	2.923 (10)	153
O8—H8*B*···N7	0.87	1.87	2.741 (11)	177

Symmetry codes: (i) x, y+1, z; (ii) x−1, y, z+1; (iii) −x+1, −y+2, −z+1; (iv) −x+1, −y+1, −z+2; (v) −x+1, −y+2, −z+2; (vi) −x+1, −y+1, −z+1; (vii) x, y, z−1; (viii) x, y−1, z.

Table S9. Hydrogen bond geometry (Å, ˚) of MMOP-**7**.

D*—H···*A	***D*—H**	**H···*A***	***D*···*A***	***D*—H···*A***
N3—H3···O3^{i}	0.84 (5)	1.88 (5)	2.715 (4)	171 (4)
O4—H4*A*···O2^{ii}	0.80 (6)	1.93 (6)	2.717 (4)	168 (5)
O4—H4*B*···O2^{iii}	0.88 (6)	2.11 (6)	2.977 (4)	168 (5)
O5—H5*A*···N1^{iv}	0.92 (6)	1.89 (6)	2.706 (4)	148 (5)
O5—H5*B*···O3^{v}	0.77 (7)	2.65 (6)	2.989 (3)	108 (5)
O5—H5*B*···N5^{v}	0.77 (7)	1.94 (7)	2.689 (4)	164 (6)
O6—H6*A*···N6	0.82 (5)	2.03 (5)	2.831 (4)	165 (4)
O6—H6*B*···O1^{vi}	0.82 (5)	2.16 (6)	2.900 (4)	150 (5)
O7—H7*A*···N7	0.85 (5)	1.88 (6)	2.731 (4)	177 (5)
O7—H7*B*···O2^{vii}	0.82 (6)	2.14 (6)	2.943 (4)	169 (5)
O8—H8*A*···N2^{vi}	0.81 (5)	1.99 (6)	2.790 (4)	169 (5)
O8—H8*B*···O1^{viii}	0.81 (5)	2.58 (5)	3.067 (3)	120 (4)
O8—H8*B*···O4^{viii}	0.81 (5)	2.27 (6)	3.030 (4)	156 (5)
O8—H8*B*···O5^{viii}	0.81 (5)	2.68 (5)	3.293 (4)	134 (4)

Symmetry codes: (i) x, y−1, z; (ii) −x+1, −y, −z+1; (iii) x, y, z−1; (iv) −x+2, −y, −z; (v) −x+2, −y+1, −z; (vi) x−1, y, z+1; (vii) x, y+1, z; (viii) −x+1, −y+1, −z+1.

Studies of Crystallinity, Purity and Homogeneity of the Bulk Samples of Metal-Organic Polymers (1-4) and Mixed Metal-Organic Polymers (5-7)

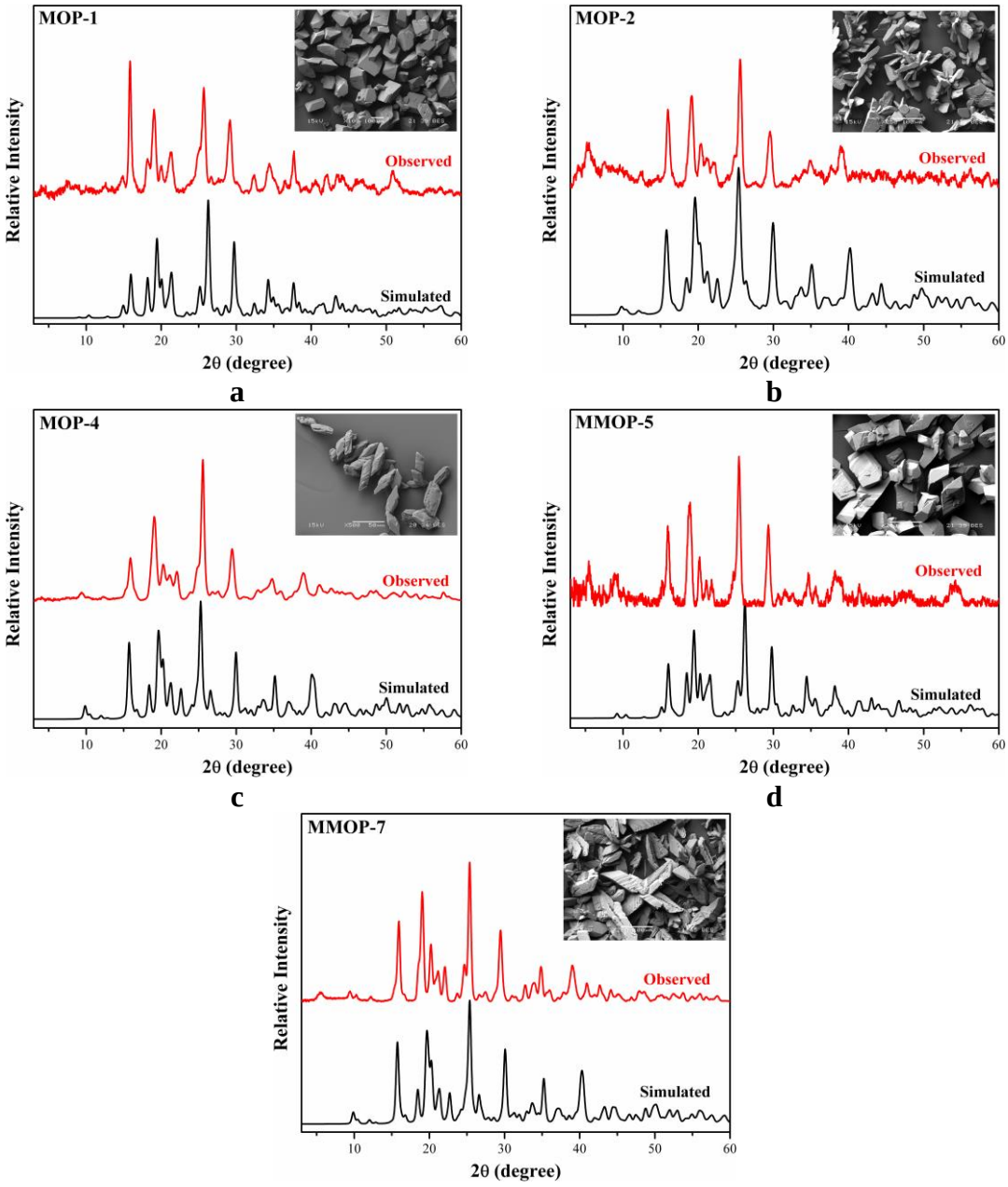

Figure S8. Characterization of MOP-**1**, MOP-**2**, MOP-**4**, MMOP-**5** and MMOP-**7** by PXRD and SEM images of the bulk crystalline samples. Scale bar 100 μm for Figure 2a-b and 2d-e, and 50 μm for Figure 2b. (a)-(e) Comparison of the observed powder X-ray diffraction with the simulated pattern calculated from the single-crystal X-ray diffraction data and the insert SEM images for each sample. Observed PXRD and simulated patterns are shown in red and black respectively.

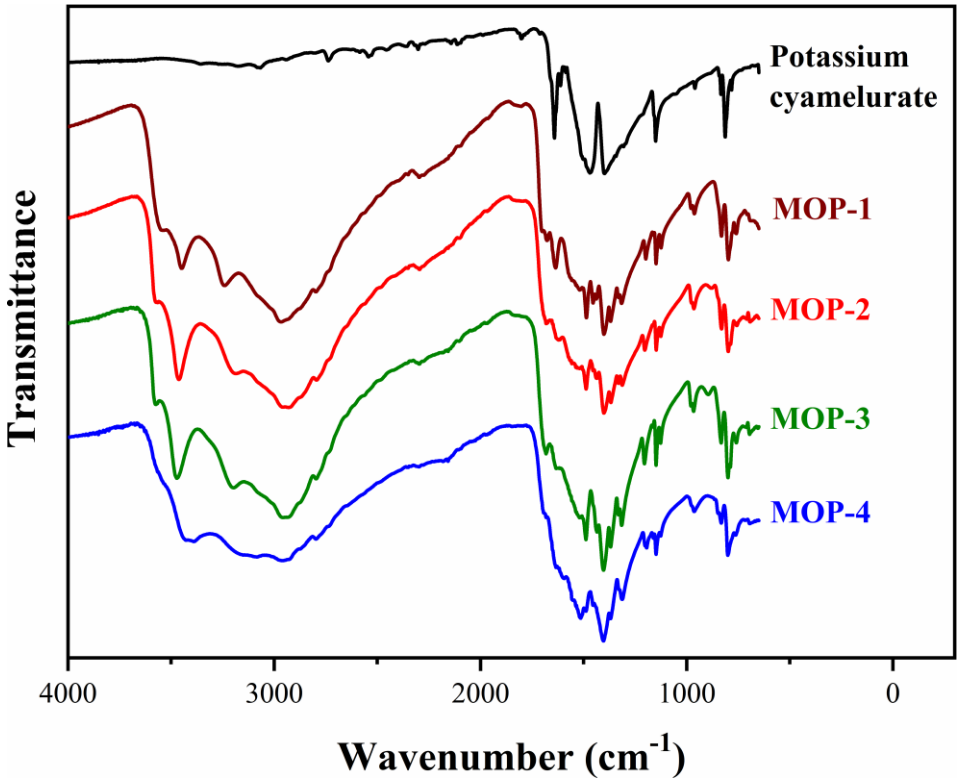

Figure S9. FT-IR spectra of MOPs-(**1-4**) compared to ligand.

Table S10. Assignment of FT-IR spectra peaks of MOPs-(**1-4**).

$\tilde{\nu}$/cm^{-1}					Assignment
Potassium cyamelurate	**MOP-1**	**MOP-2**	**MOP-3**	**MOP-4**	
	693sh 709sh	692sh 709sh	695sh 708sh	694sh	Ring breathing, τ(OH)
	760w	755sh	760sh	762sh	τ(OH)
782w 814m	777w 798w	787w 799w	768w 788w 800w	 801w	γ(CN)-Linker, Ring Breathing for all, τ(NH), ω(OH)-MOPs
834w	832w	831w	833w	833w 848sh	Ring Breathing for all, ν(CN) saturated N atom-linker, ω(OH)-MOPs
961w	963w	966w	967w	964w	(Ring Breathing, ν(CN) in ring-linker), (ρ(OH) hydrogen-bonded, γ(CN), ω(NH)-MOPs)
 1150m	1121w 1149w 1162w	1126w 1148w	1127w 1149w 1165w	1127w 1149w 1161w	ν(CN) in ring for all, ρ(OH)-MOPs
	1199w	1204w	1205w	1195w 1203w	Ring Breathing, ρ(OH)
1310sh	1317w 1333w	1313w 1333w	1316w 1331w	1313w 1330w	ν(CN) in ring for all, ρ(NH)-MOPs
	1370m	1368m	1369m	1369w	Ring breathing, δ(OH)
1399s	1402s 1438w	1402s 1436vw	1404s 1436w	1404s	ν(CN)-linker, δ(OH)-MOPs
1470s	1455w 1487m	1488m	1489	1454w 1486w	δ(OH)-MOPs, ν(CN)-Linker
1503s					ν(CN) in ring-linker
1586vw					ν(CN) in ring for all, ρ(NH)
	1636w		1635sh	1634sh	ω(NH), Ring Breathing
1642m				1635sh	ν(CO) single bond type-linker
	1677sh 1701sh	1680sh	1683sh		ν(CO) double bond type-MOPs
1801w					ν(CO) double bond type-linker (due to resonance)
	2798sh 2965s	2790sh 2930s	2796sh 2957s	2797sh 2957m	ν(OH) (hydrogen-bonded)
	3240w 3450w 3547w	3193m 3463m 3579sh	3201w 3473w 3576sh	3085w 3390w 3430m	ν(NH) (characteristic amide)

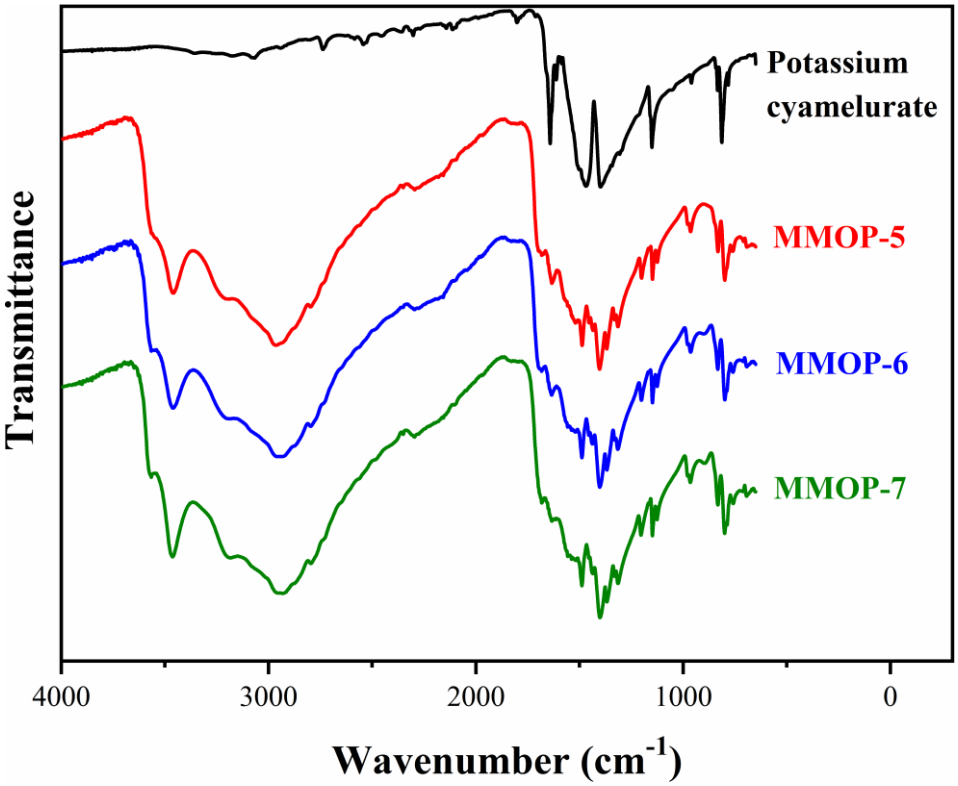

Figure S10. FT-IR spectra of MMOPs-(**5-7**) compared to ligand.

Table S11. Assignment of FT-IR spectra peaks of MMOPs-(**5-7**).

$\tilde{\nu}$/cm^{-1}				Assignment
Potassium cyamelurate	**MMOP-5**	**MMOP-6**	**MMOP-7**	
	691sh	693sh	694sh	
	709sh	709sh	708sh	Ring breathing, τ(OH)
	761sh	760sh	759sh	τ(OH)
782w	788sh	787sh	767sh	
814m	799w	799sh	788w	γ(CN)-Linker, Ring Breathing for all,
			800w	τ(NH), ω(OH)-MMOPs
834w	832w	833w	833w	Ring Breathing for all, ν(CN) saturated N atom-linker, ω(OH)-MMOPs
961w	964w	964w	966w	(Ring Breathing, ν(CN) in ring-linker), (ρ(OH) hydrogen-bonded, γ(CN),
1051sh	977w	978w	979w	ω(NH)-MMOPs)
	1125w	1126w	1126w	ν(CN) in ring for all, ρ(OH)-MOPs
	1148w	1148w	1148w	
1150m	1161sh	1163sh	1163sh	
	1201w	1202w	1204w	Ring Breathing, ρ(OH)
1310sh	1315w	1316w	1315w	
	1331w	1329w	1330w	
	1369w	1369m	1368m	ν(CN) in ring for all, ρ(NH)-MOPs
1399s	1404s	1403s	1402s	Ring breathing, δ(OH)
	1435w	1438w	1438w	
1470s	1455w	1454w	1455w	ν(CN)-linker, δ(OH)-MOPs
	1488w	1489w	1489w	
1503s				δ(OH)-MOPs, ν(CN)-Linker
1586vw				ν(CN) in ring-linker
1613w				ν(CN) in ring for all, ρ(NH)
	1634w	1635w	1633w	
1642m				ω(NH), Ring Breathing
	1682w	1682w	1682w	ν(CO) single bond type-linker
	1699sh			
1801w				ν(CO) double bond type-MOPs
	2794sh	2793sh	2790sh	ν(CO) double bond type-linker (due to
	2964m	2958s	2934s	resonance)
				ν(OH) (hydrogen-bonded)
	3216m	3207m	3192m	
	3459m	3462m	3463m	ν(NH) (characteristic amide)
	3567sh	3565sh	3564sh	

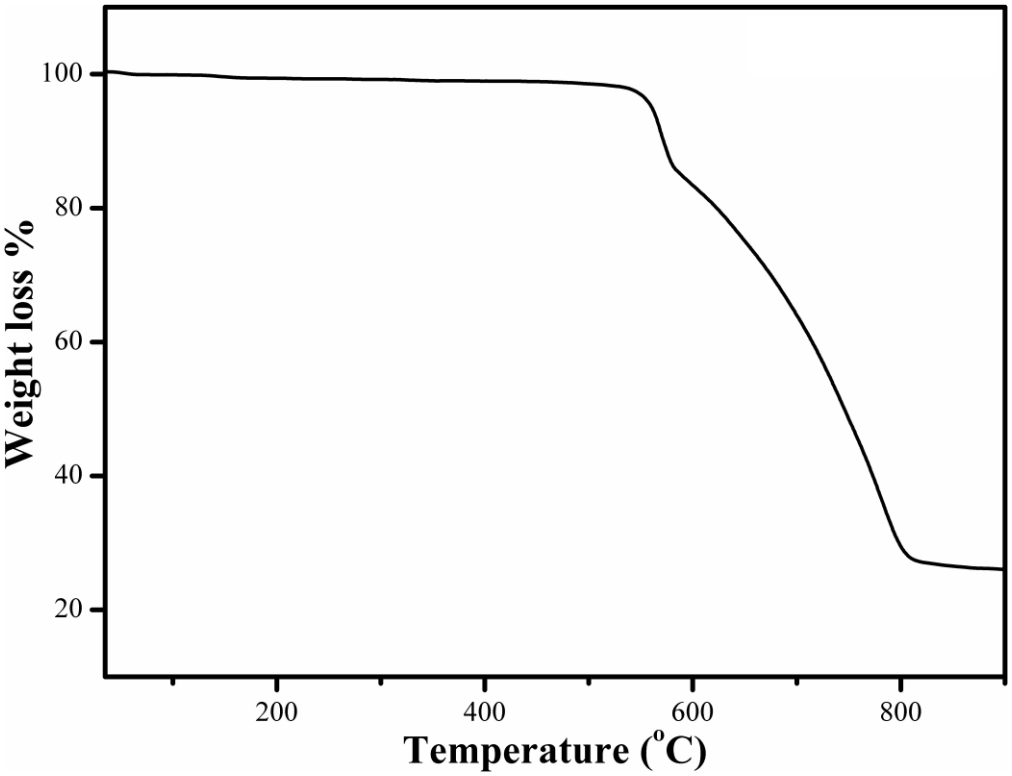

Figure S11. Thermogravimetric analysis curve of cyamelurate.

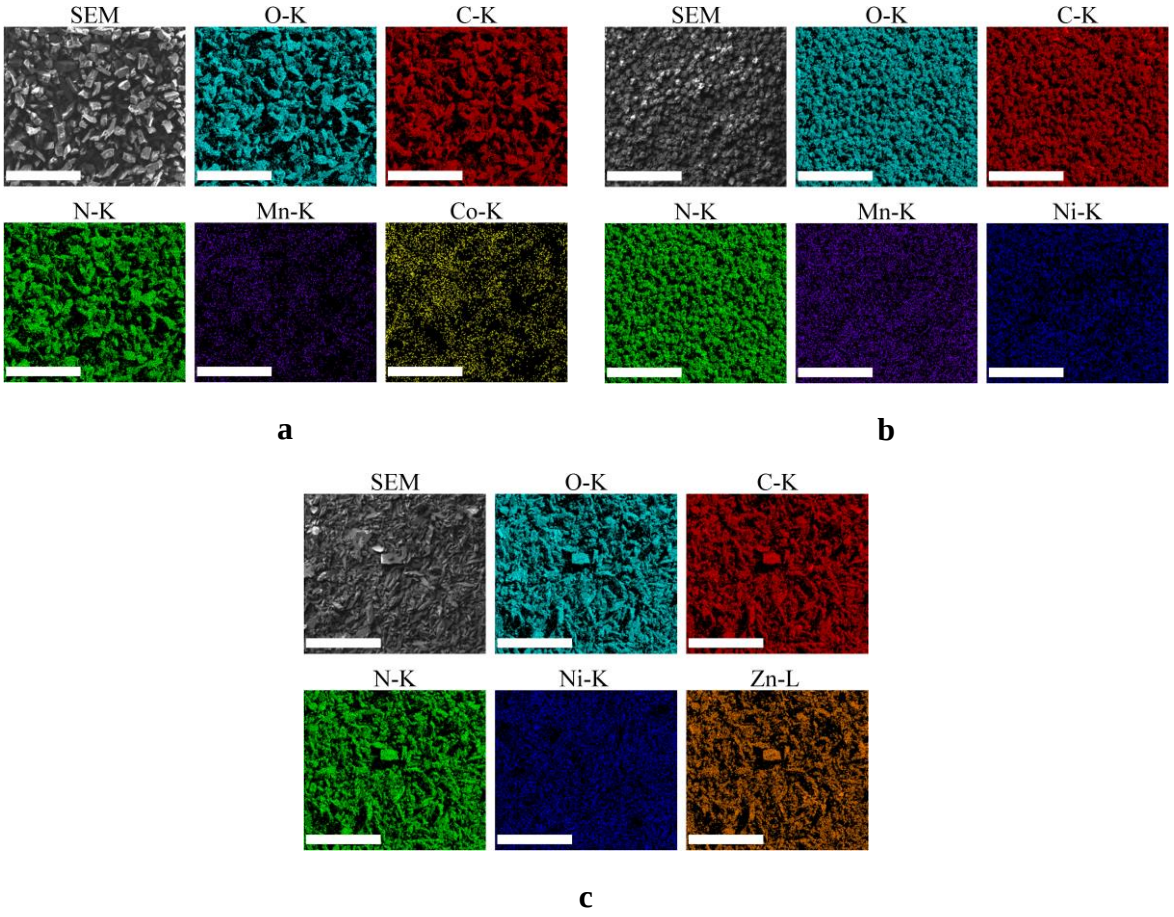

Figure S12. Energy Dispersive X-ray Diffraction analyses of MMOP-(**5-7)**. (a)-(c) EDS element-mapping images of MMOPs-(**5-7**) respectively, showing the distribution of carbon (red), nitrogen (green), oxygen (cyan) and metal ions (Mn in purple, Co in yellow, Ni in blue and Zn in orange) in the area of the crystalline samples (scale bar, 500 μm).

In-situ Energy Dispersive Spectroscopy/Scanning Electron Microscopy

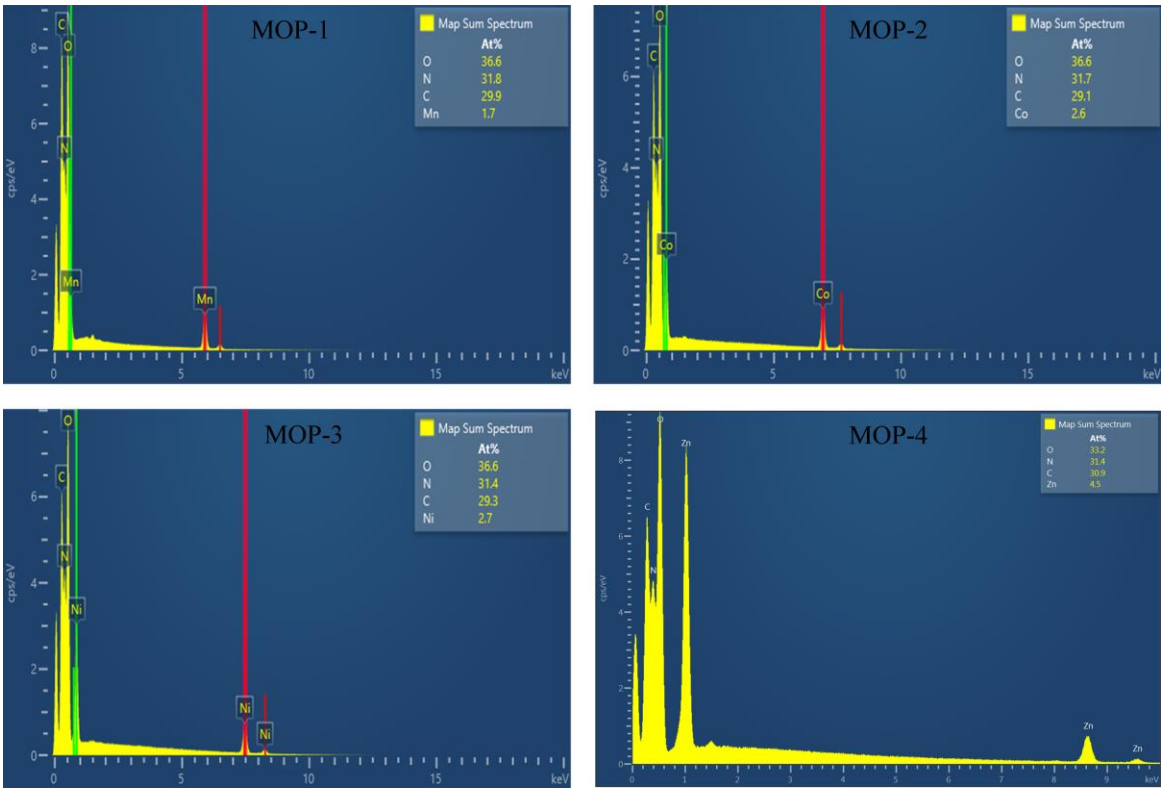

Figure S13. Energy Dispersive X-ray Diffraction plot analysis of MOPs-(**1-4**) representing the percentage of elements.

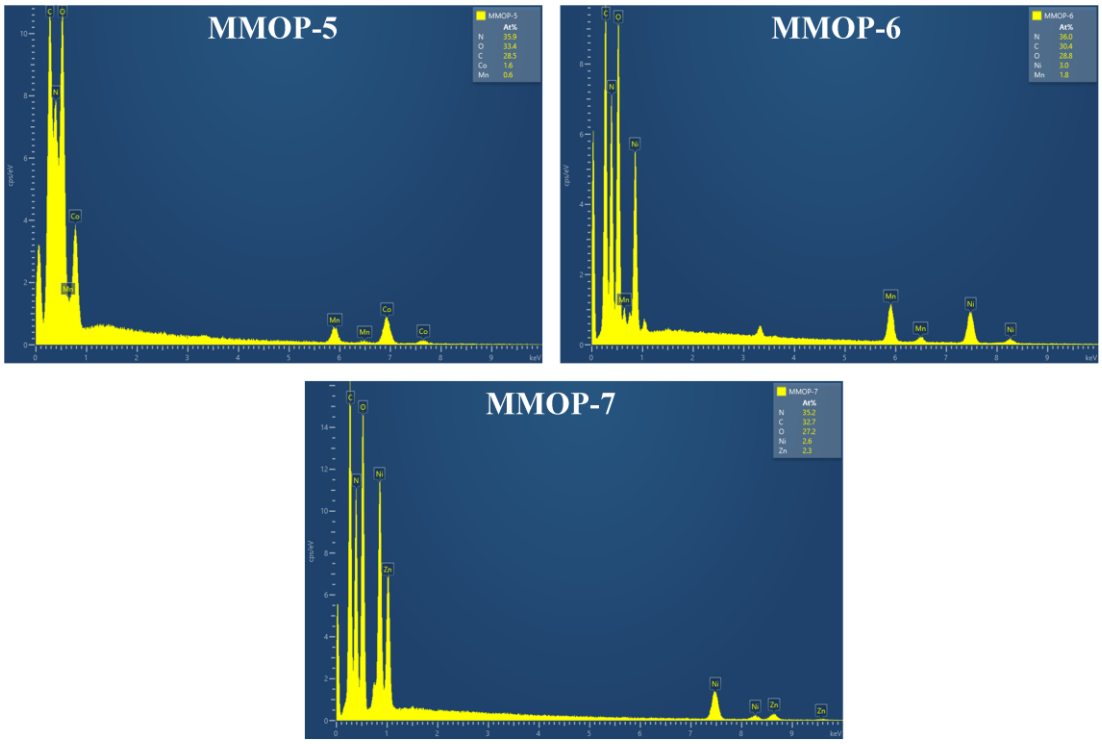

a

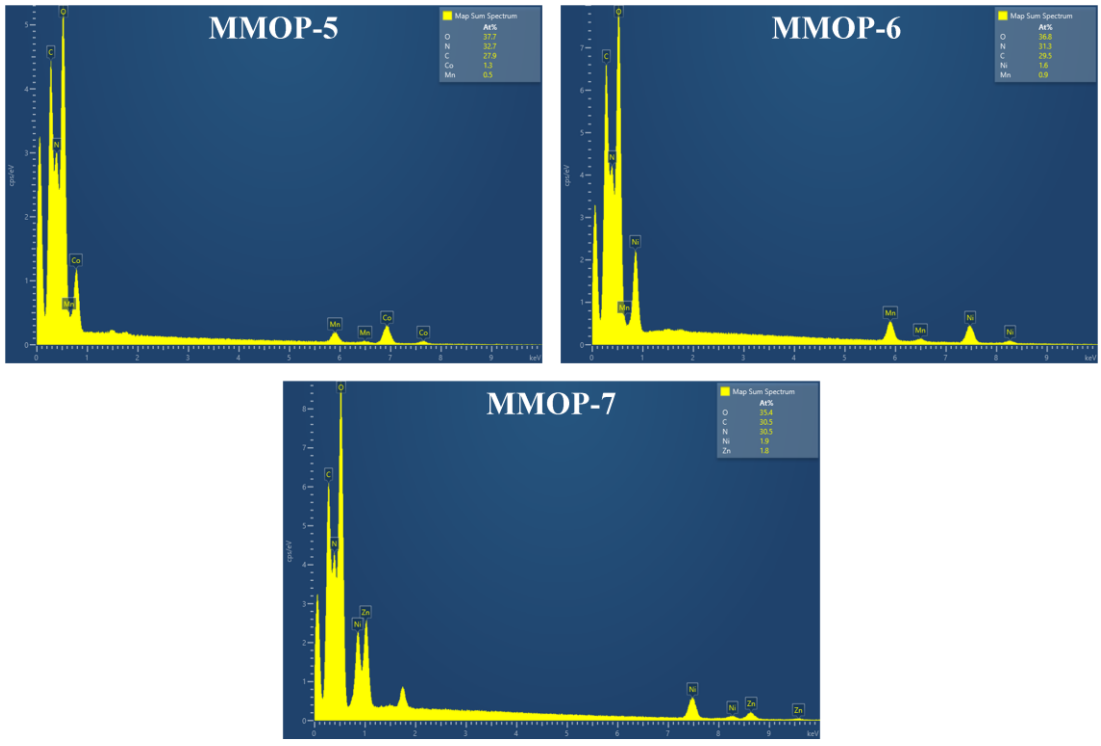

b

Figure S14. Energy Dispersive X-ray Diffraction plot analysis of MMOPs-(**5-7**) representing the percentage of elements. a) Point, b) Mapping analysis.

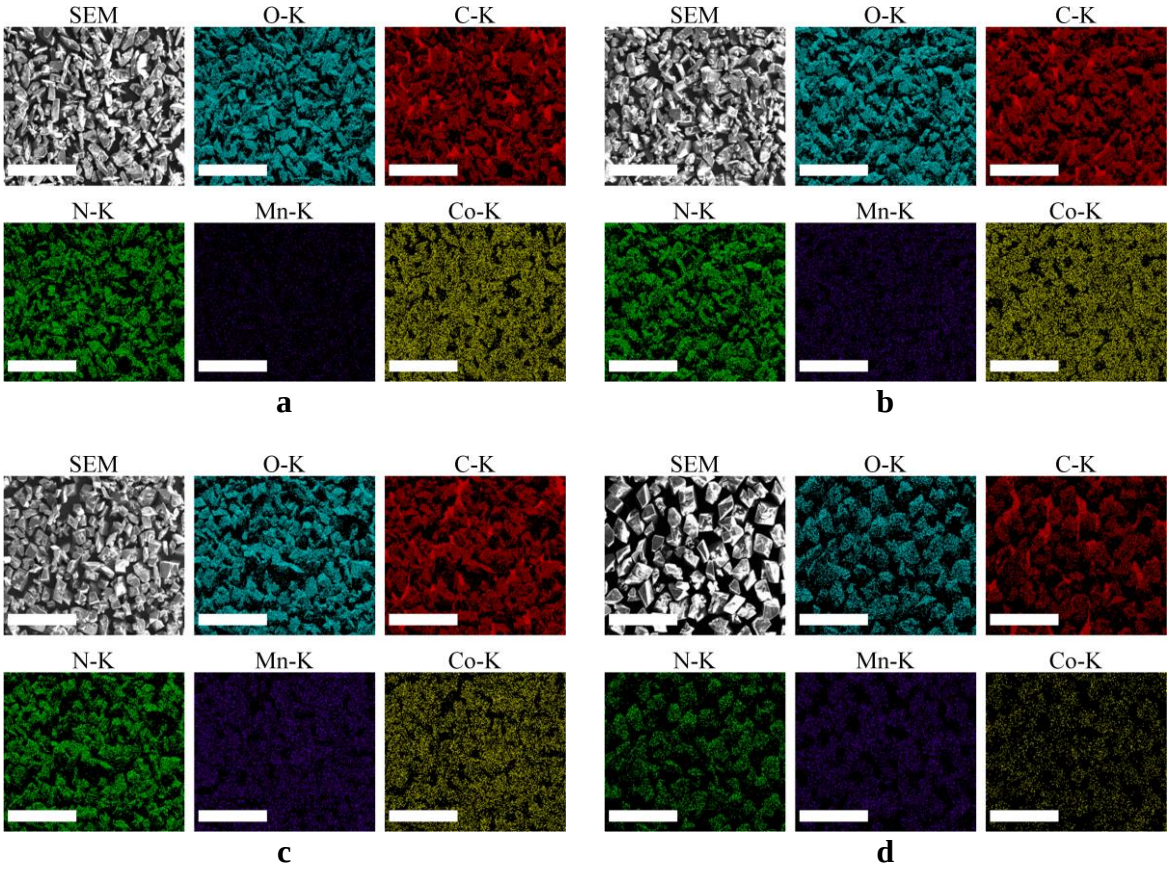

Figure S15. Energy Dispersive X-ray Diffraction mapping analysis of MMOP-**5** metal ratios study. a)20-80, b) 40-60, c) 60-40, d) 80-20 (Scale bar, 500 μm).

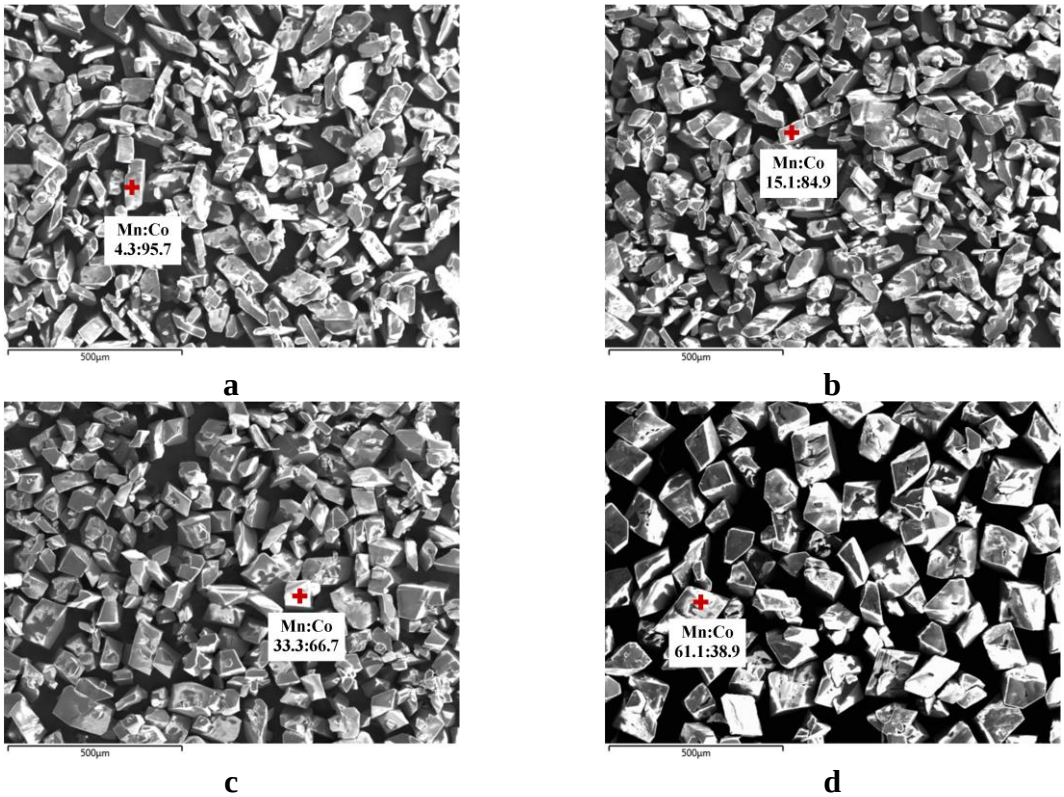

Figure S16. Energy Dispersive X-ray Diffraction point analysis of MMOP-**5** metal ratios study. a) 20-80, b) 40-60, c) 60-40, d) 80-20.

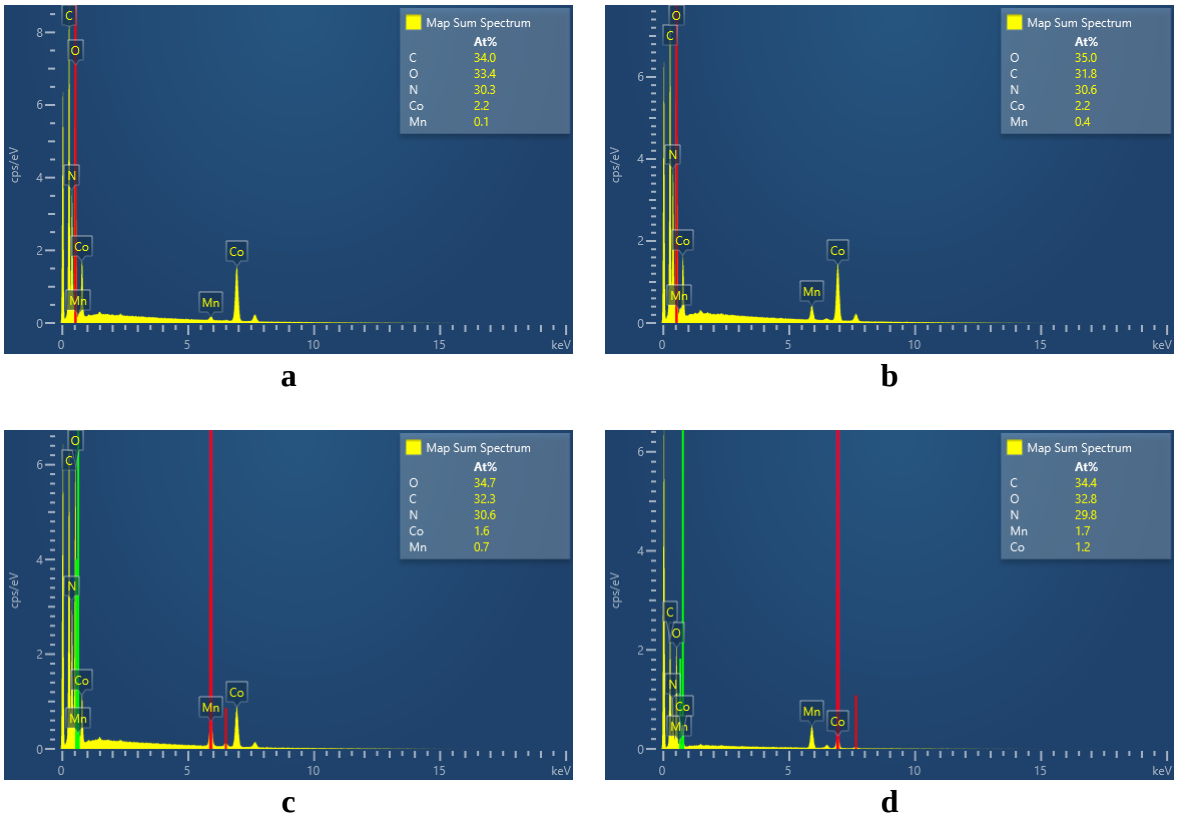

Figure S17. Energy Dispersive X-ray Diffraction plot of mapping analysis of MMOP-5 metal ratio study a) 20-80, b) 40-60, c) 60-40, d) 80-20.

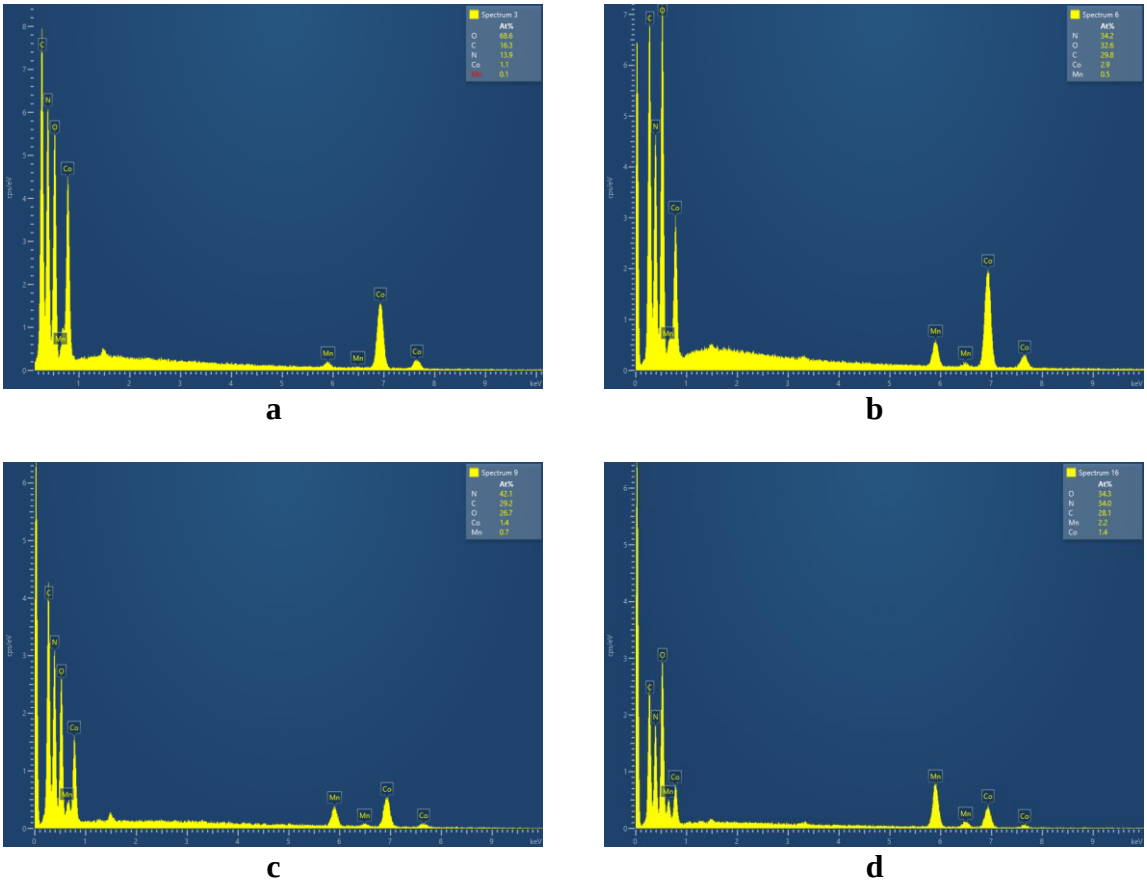

Figure S18. Energy Dispersive X-ray Diffraction plot of point analysis of MMOP-5 metal ratio study a) 20-80, b) 40-60, c) 60-40, d) 80-20.

Table S12. Summary of Energy Dispersive X-ray Diffraction analysis of MMOP-**5** prepared with different metal ratios.

Ratios	**Ratios seen in EDS (Mn:Co)**	
	Mole %	
	Mapping	**Point**
20:80	4.3:95.7	4.3:95.7
40:60	15.4:84.6	15.1:84.9
50:50	28:72	28:72
60:40	30.4:69.6	33.3:66.7
80:20	58.6:41.4	61.1:38.9

X-ray photoelectron spectroscopy

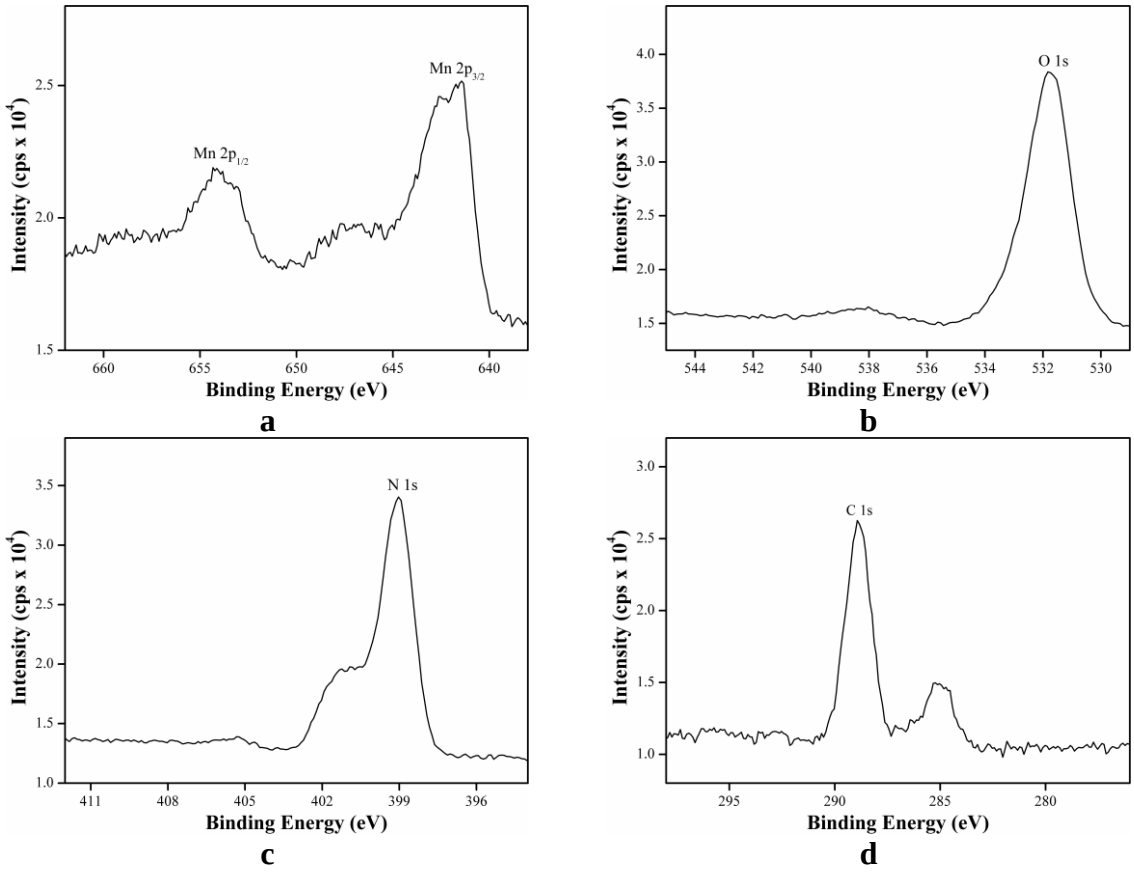

Figure S19. XPS patterns of MOP-**1**. a)-d) Narrow survey XPS in MOP-**1** of Mn $2p_{3/2}$ and $2p_{1/2}$; O 1s; N 1s; C 1s.

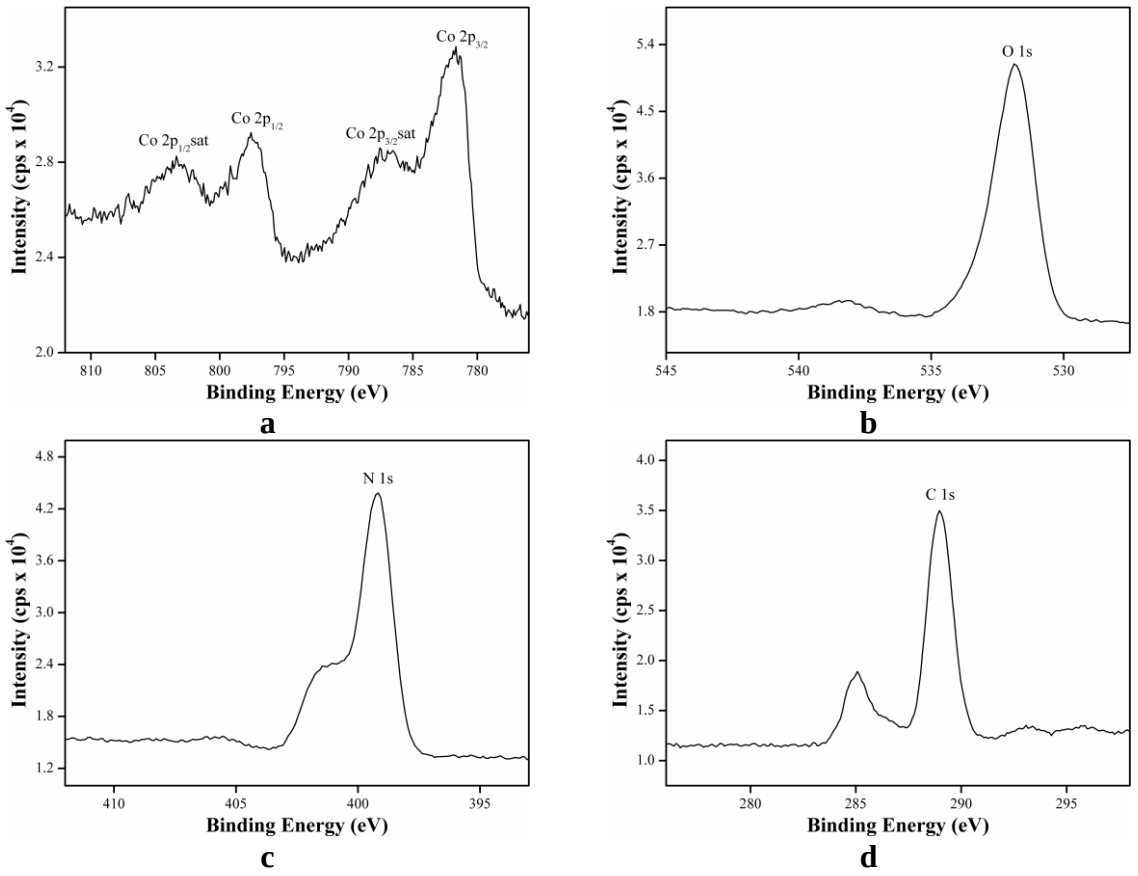

Figure S20. XPS patterns of MOP-**2**. a)-d) Narrow survey XPS in MOP-**2** of Co $2p_{3/2}$, $2p_{3/2}$sat, $2p_{1/2}$ and $2p_{1/2}$sat; O 1s; N 1s; C 1s.

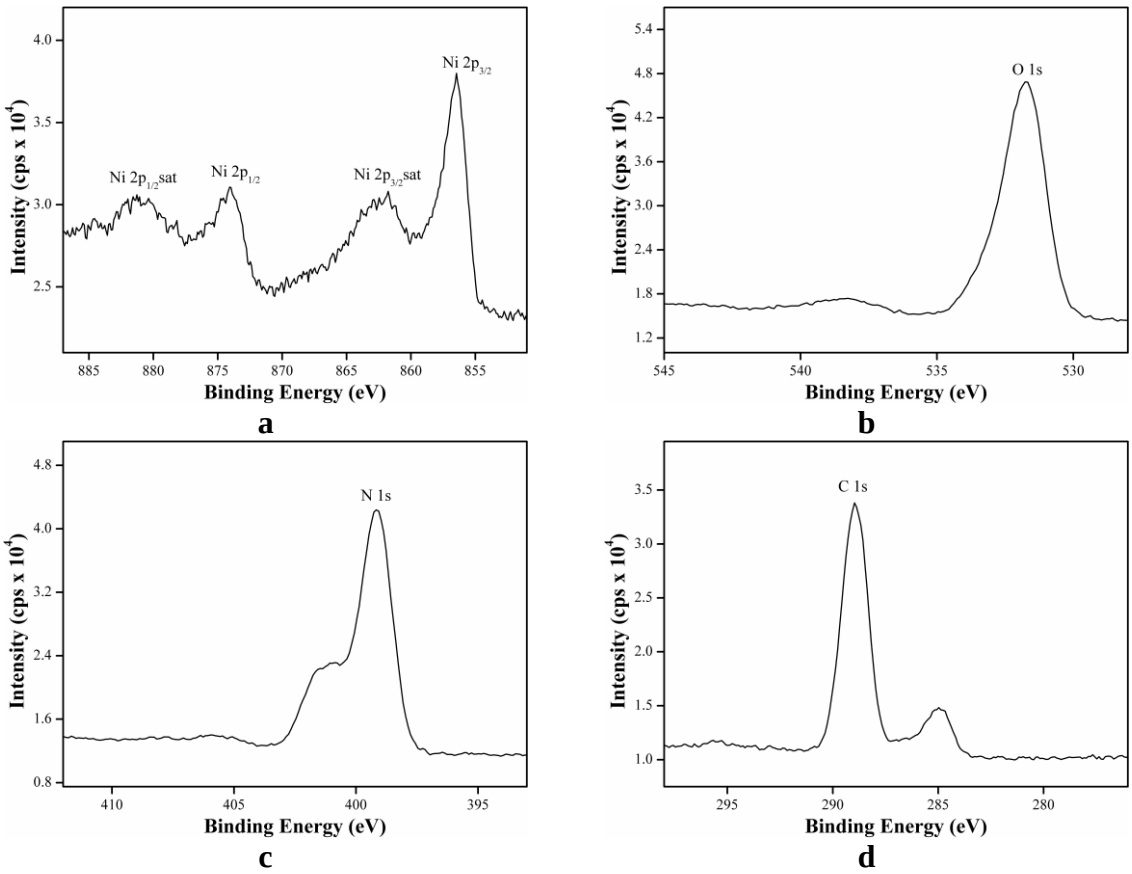

Figure S21. XPS patterns of MOP-**3**. a)-d) Narrow survey XPS in MOP-**3** of Ni $2p_{3/2}$, $2p_{3/2}$sat, $2p_{1/2}$ and $2p_{1/2}$sat; O 1s; N 1s; C 1s.

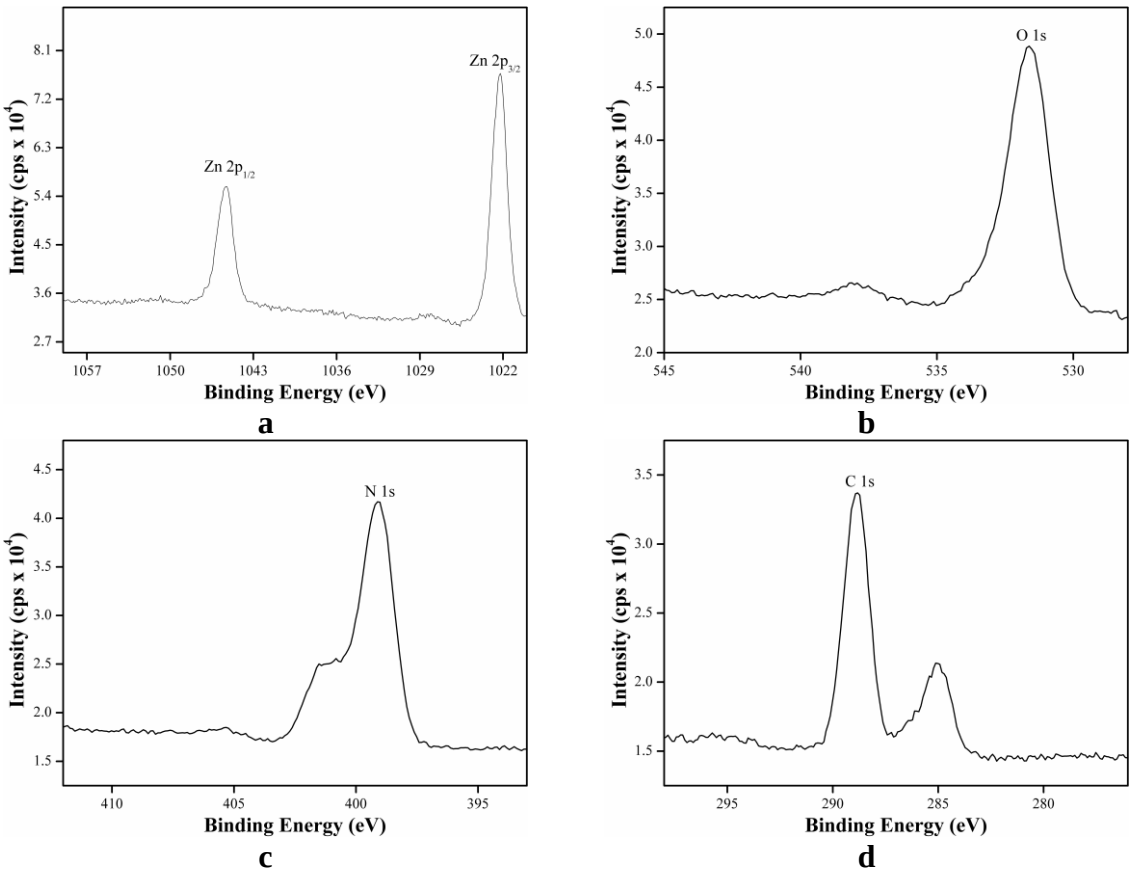

Figure S22. XPS patterns of MOP-**4**. a)-d) Narrow survey XPS in MOP-**4** of Zn $2p_{3/2}$ and $2p_{1/2}$; O 1s; N 1s; C 1s.

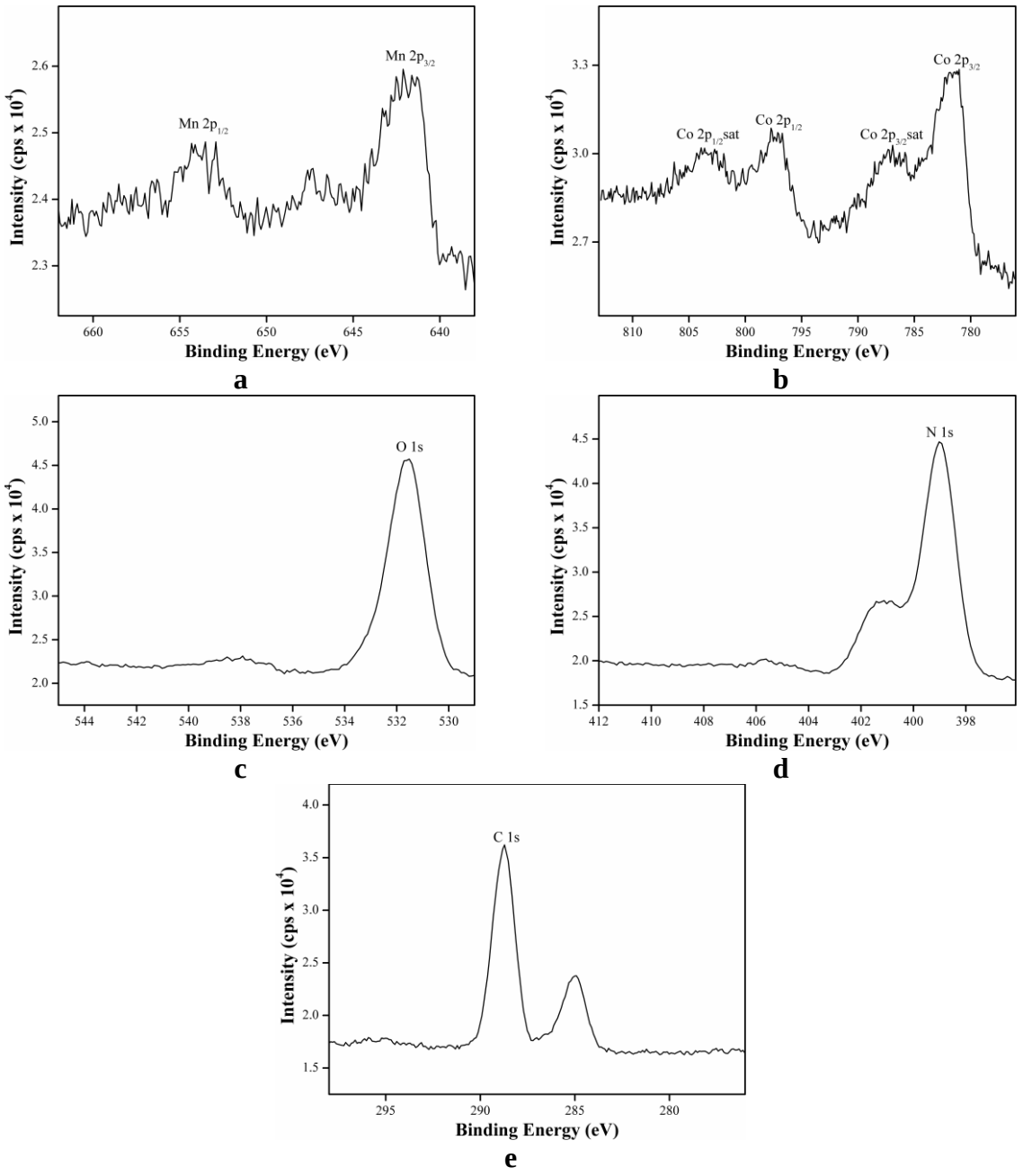

Figure S23. XPS patterns of MMOP-**5**. a)-e) Narrow survey XPS in MMOP-**5** of Mn $2p_{3/2}$ and $2p_{1/2}$; Co $2p_{3/2}$, $2p_{3/2}$sat, $2p_{1/2}$ and $2p_{1/2}$sat; O 1s; N1s; C 1s.

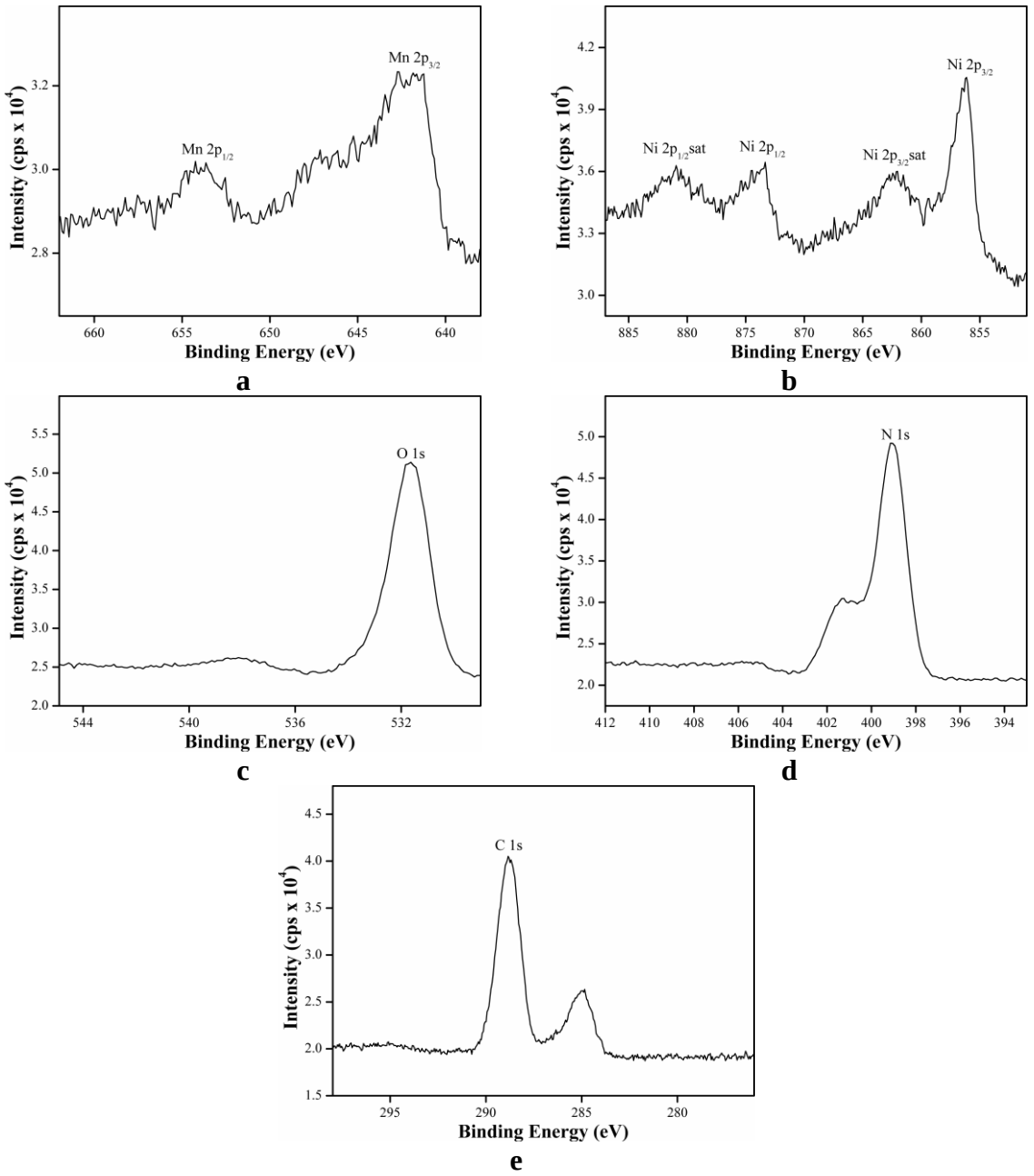

Figure S24. XPS patterns of MMOP-**6**. a)-e) Narrow survey XPS in MMOP-**6** of Mn $2p_{3/2}$ and $2p_{1/2}$; Ni $2p_{3/2}$, $2p_{3/2}$sat, $2p_{1/2}$ and $2p_{1/2}$sat; O 1s; N1s; C 1s.

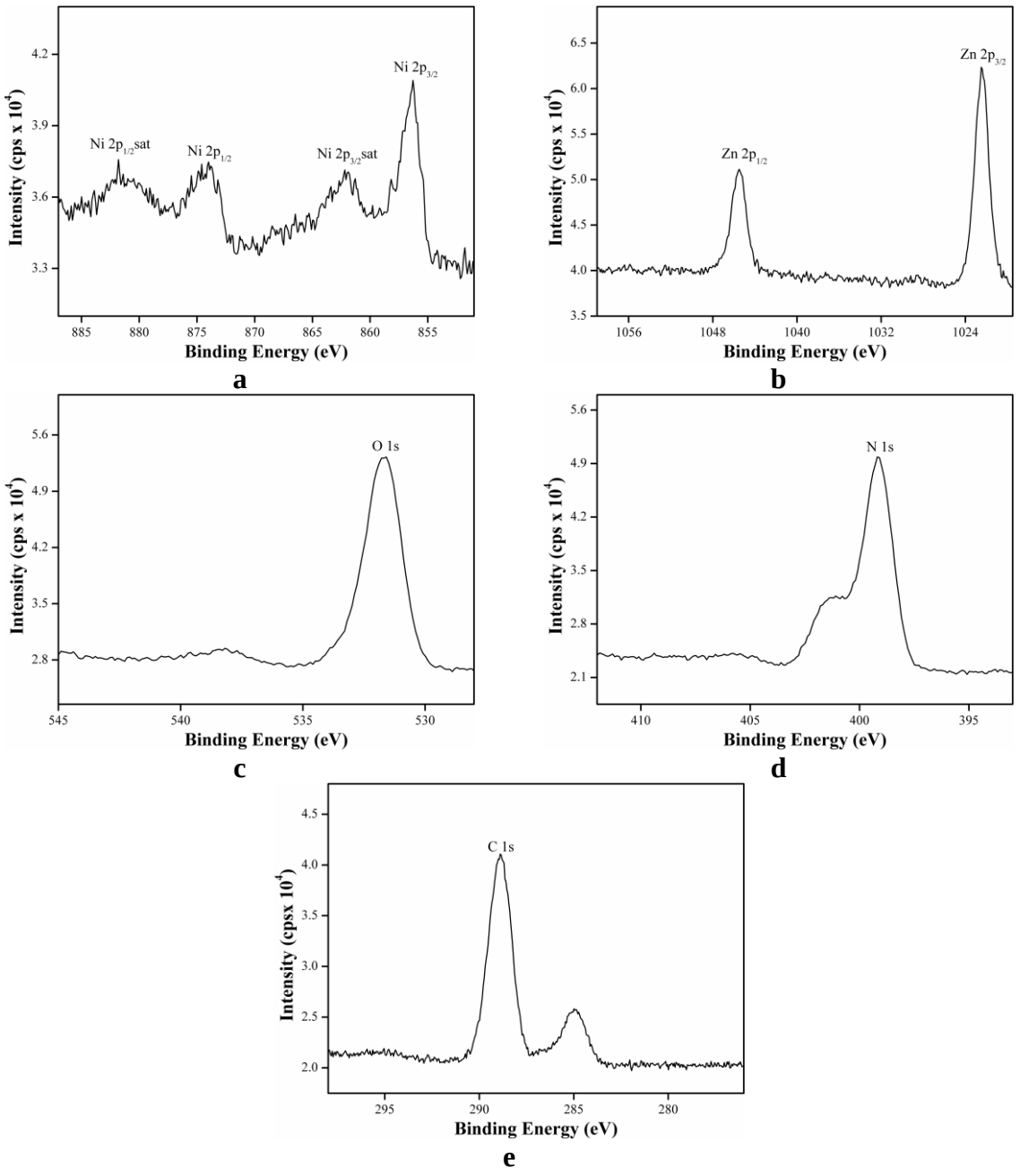

Figure S25. XPS patterns of MMOP-**7**. a)-e) Narrow survey XPS in MMOP-**7** of Ni $2p_{3/2}$, $2p_{3/2}$sat, $2p_{1/2}$ and $2p_{1/2}$sat; Zn $2p_{3/2}$ and $2p_{1/2}$; O 1s; N1s; C 1s.

Table S13. Binding energy values (eV) of XPS elements peaks for MOPs-(**1-4**) and MMOPs-(**5-7**).

Element / Sample	Mn		Co				Ni				Zn		O	N	C
	$2p_{1/2}$	$2p_{3/2}$	$2p_{1/2sat}$	$2p_{1/2}$	$2p_{3/2sat}$	$2p_{3/2}$	$2p_{1/2sat}$	$2p_{1/2}$	$2p_{3/2sat}$	$2p_{3/2}$	$2p_{3/2}$	$2p_{1/2}$	1s	1s	1s
MOP-1	654	641		-				-			-		531	399	288
MOP-2	-		804	797	786	782		-			-		531	399	288
MOP-3	-			-			881	873	862	856			531	399	288
MOP-4	-			-				-			1022	1045	531	399	288
MMOP-5	654	641	804	797	786	782		-			-		531	399	288
MMOP-6	654	641		-			881	873	862	856	-		531	399	288
MMOP-7				-			881	873	862	856	1022	1045	531	399	288

Studies of Chromic Behaviour and Structural Transformation

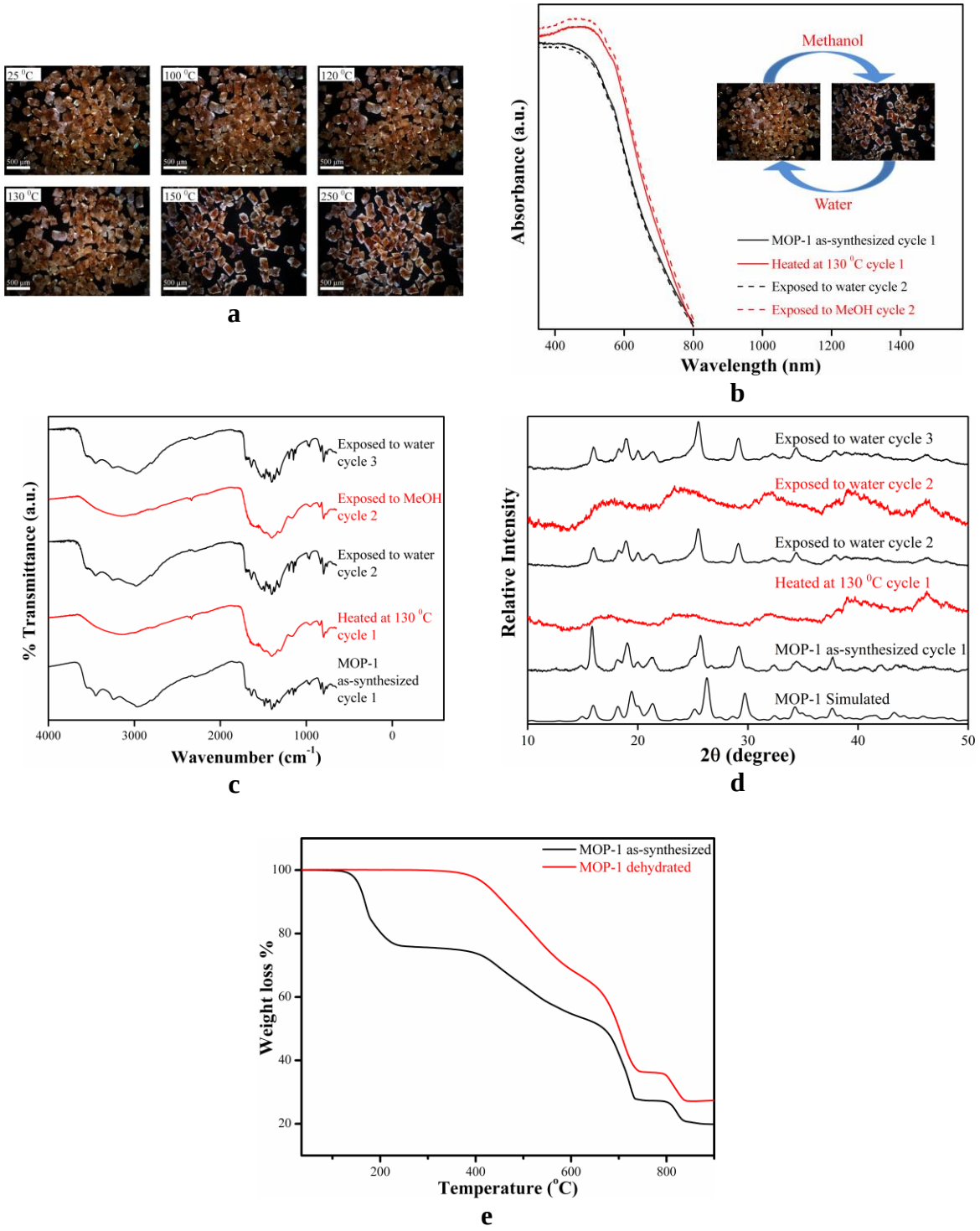

Figure S26. Chromic behaviour analysis of MOP-**1** using a) *In-situ* thermal microscopy images at different temperatures from 25-250 ºC (scale bar: 500 µm); b) UV-Vis spectra changes for MOP-**1**. Black solid lines: MOP-**1** as synthesized; red solid lines: heated at 130 ºC, black dash lines: sample on exposure in water and red dash lines: sample on exposure in methanol. Insert: chromism images of MOP-**1**; c) FTIR spectra of the MOP-**1** as-synthesized, heated at 130 ºC, exposed to water and then exposed to methanol d) PXRD patterns of the samples taken at different cycles and the simulated patterns calculated from the single-crystal X-ray diffraction data. e) TG curves of MOP-**1** as synthesized and dehydrated. One cycle is referred to a process of dehydration followed by hydration.

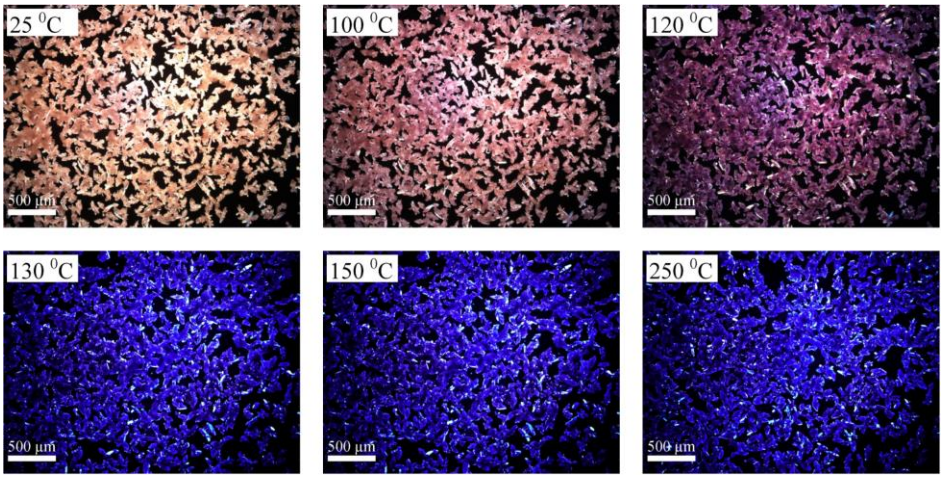

Figure S27. Chromic behaviour analysis of MOP-**2** using *in-situ* thermal microscopy images at different temperatures from 25-250 ºC (scale bar: 500 µm).

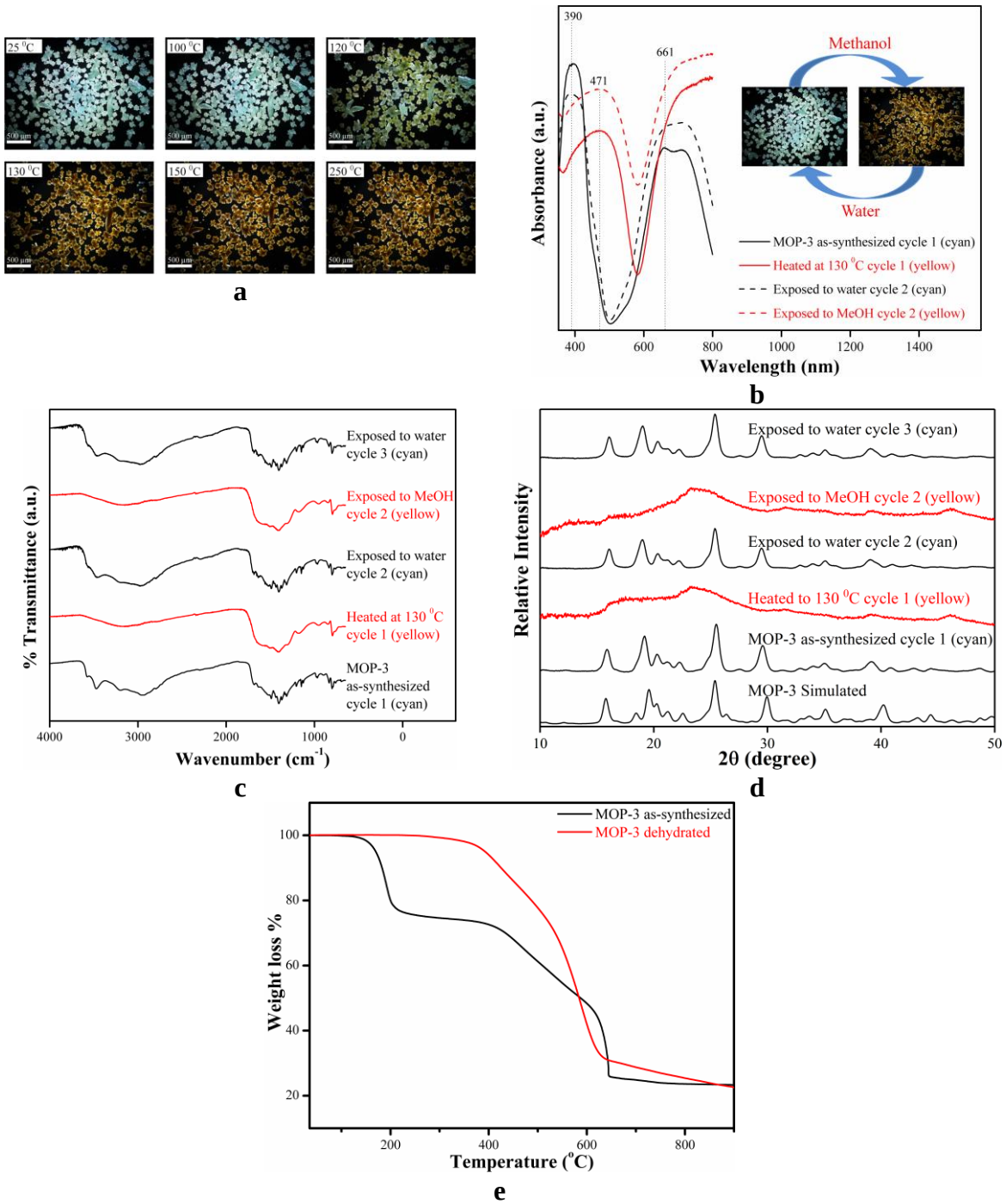

Figure S28. Chromic behaviour analysis of MOP-**3** using. a) *In-situ* thermal microscopy images at different temperatures from 25-250 ºC (scale bar: 500 µm); b) UV-Vis spectra changes for MOP-**3**. Black solid lines: MOP-**3** as synthesized; red solid lines: heated at 130 ºC, black dash lines: sample on exposure in water and red dash lines: sample on exposure in methanol. Insert: chromism images of MOP-**3**; c) FTIR spectra of the MOP-**3** as-synthesized, heated at 130 ºC, exposed to water and then exposed to methanol d) PXRD patterns of the samples taken at different cycles and the simulated patterns calculated from the single-crystal X-ray diffraction data. e) TG curves of MOP-**3** as synthesized and dehydrated. One cycle is referred to a transformation that bring the cyan species to yellow species and return to the original colour.

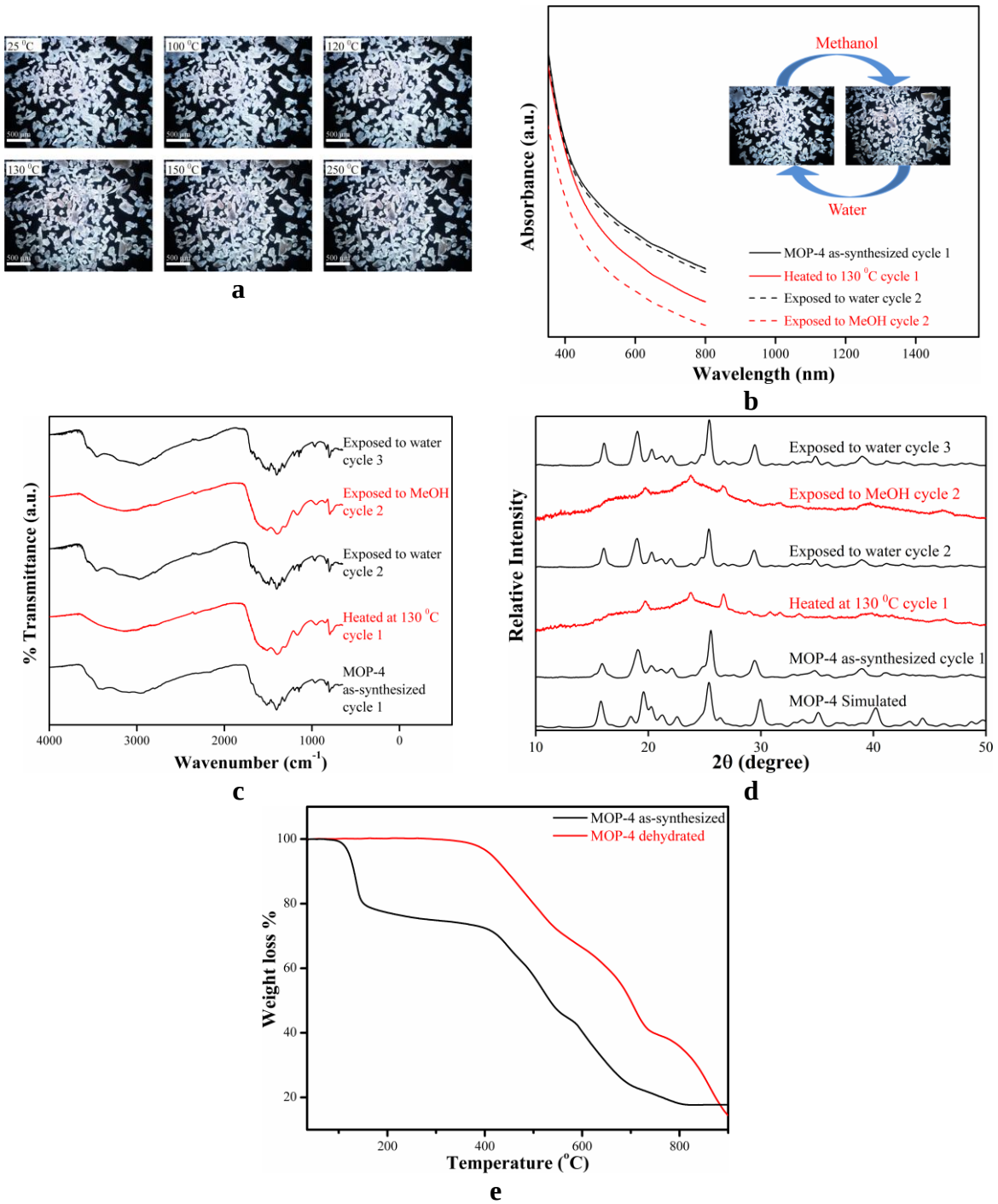

Figure S29. Chromic behaviour analysis of MOP-**4** using. a) *In-situ* thermal microscopy images at different temperatures from 25-250 ºC (scale bar: 500 μm); b) UV-Vis spectra changes for MOP-**4**. Black solid lines: MOP-**4** as synthesized; red solid lines: heated at 130 ºC, black dash lines: sample on exposure in water and red dash lines: sample on exposure in methanol. Insert: chromism images of MOP-**4**; c) FTIR spectra of the MOP-**4** as-synthesized, heated at 130 ºC, exposed to water and then exposed to methanol d) PXRD patterns of the samples taken at different cycles and the simulated patterns calculated from the single-crystal X-ray diffraction data. e) TG curves of MOP-**4** as synthesized and dehydrated. One cycle is referred to a process of dehydration followed by hydration.

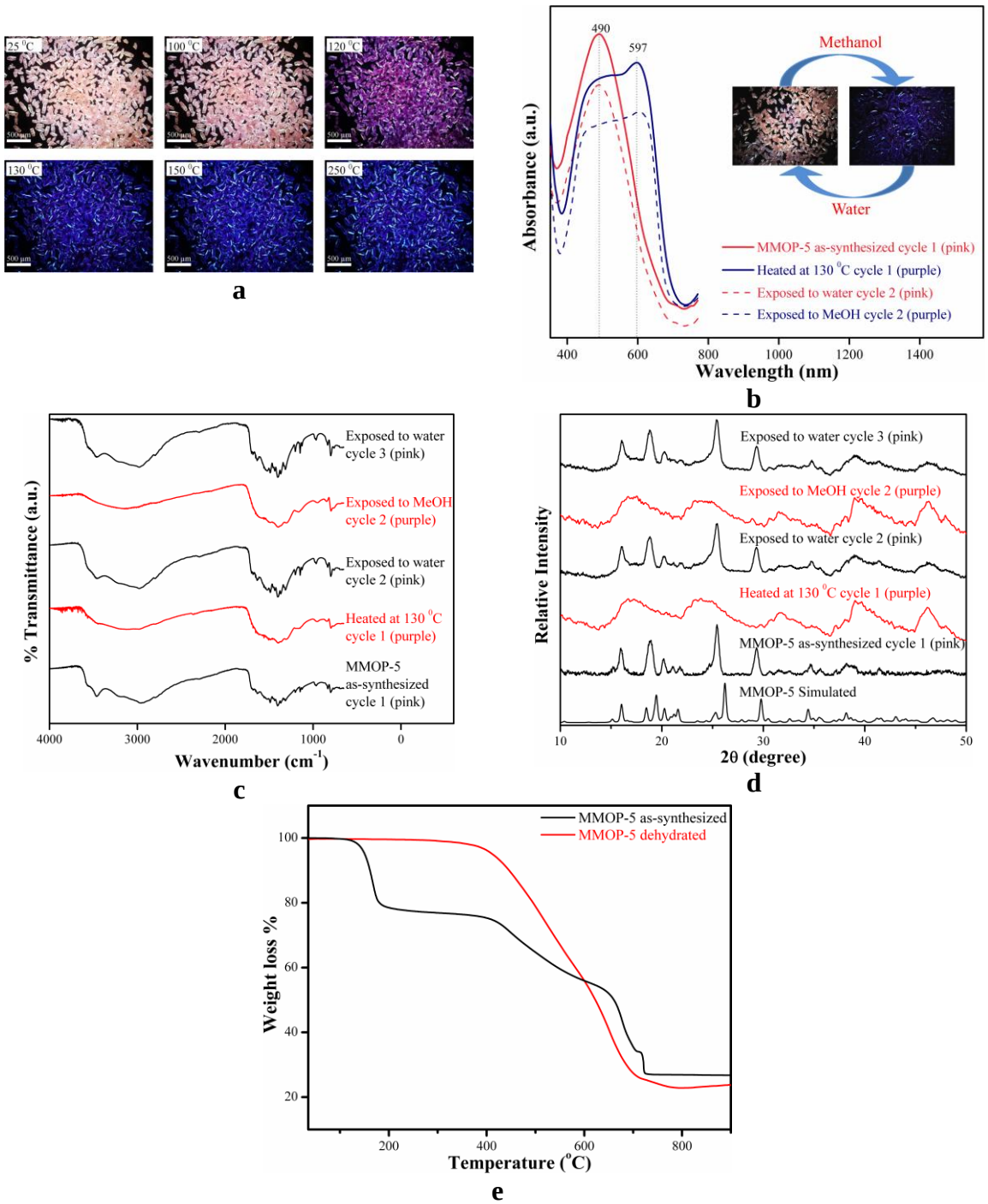

Figure S30. Chromic behaviour analysis of MMOP-**5** using. a) *In-situ* thermal microscopy images at different temperatures from 25-250 ºC (scale bar: 500 µm); b) UV-Vis spectra changes for MMOP-**5**. Pink solid lines: MMOP-**5** as synthesized; purple solid lines: heated at 130 ºC, pink dash lines: sample on exposure in water and purple dash lines: sample on exposure in methanol. Insert: chromism images of MMOP-**5**; c) FTIR spectra of the MMOP-**5** as-synthesized, heated at 130 ºC, exposed to water and then exposed to methanol d) PXRD patterns of the samples taken at different cycles and the simulated patterns calculated from the single-crystal X-ray diffraction data. e) TG curves of MMOP-**5** as synthesized and dehydrated. One cycle is referred to a transformation that bring the pink species to purple species and return to the original colour.

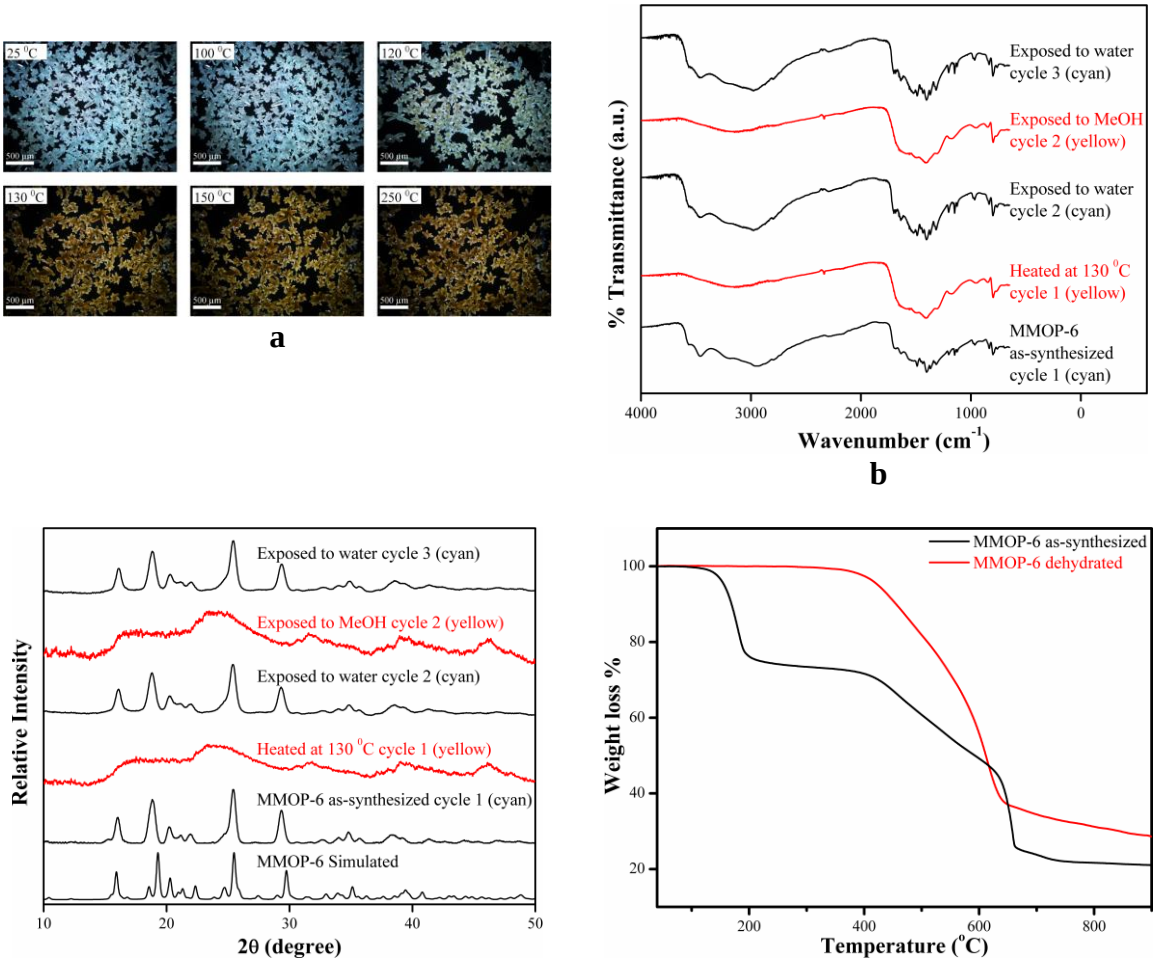

Figure S31. Chromic behaviour analysis of MMOP-**6** using. a) *In-situ* thermal microscopy images at different temperatures from 25-250 ºC (scale bar: 500 µm); b) FTIR spectra of the MMOP-**6** as-synthesized, heated at 130 ºC, exposed to water and then exposed to methanol c) PXRD patterns of the samples taken at different cycles and the simulated patterns calculated from the single-crystal X-ray diffraction data. d) TG curves of MMOP-**6** as synthesized and dehydrated. One cycle is referred to a transformation that bring the cyan species to yellow species and return to the original colour.

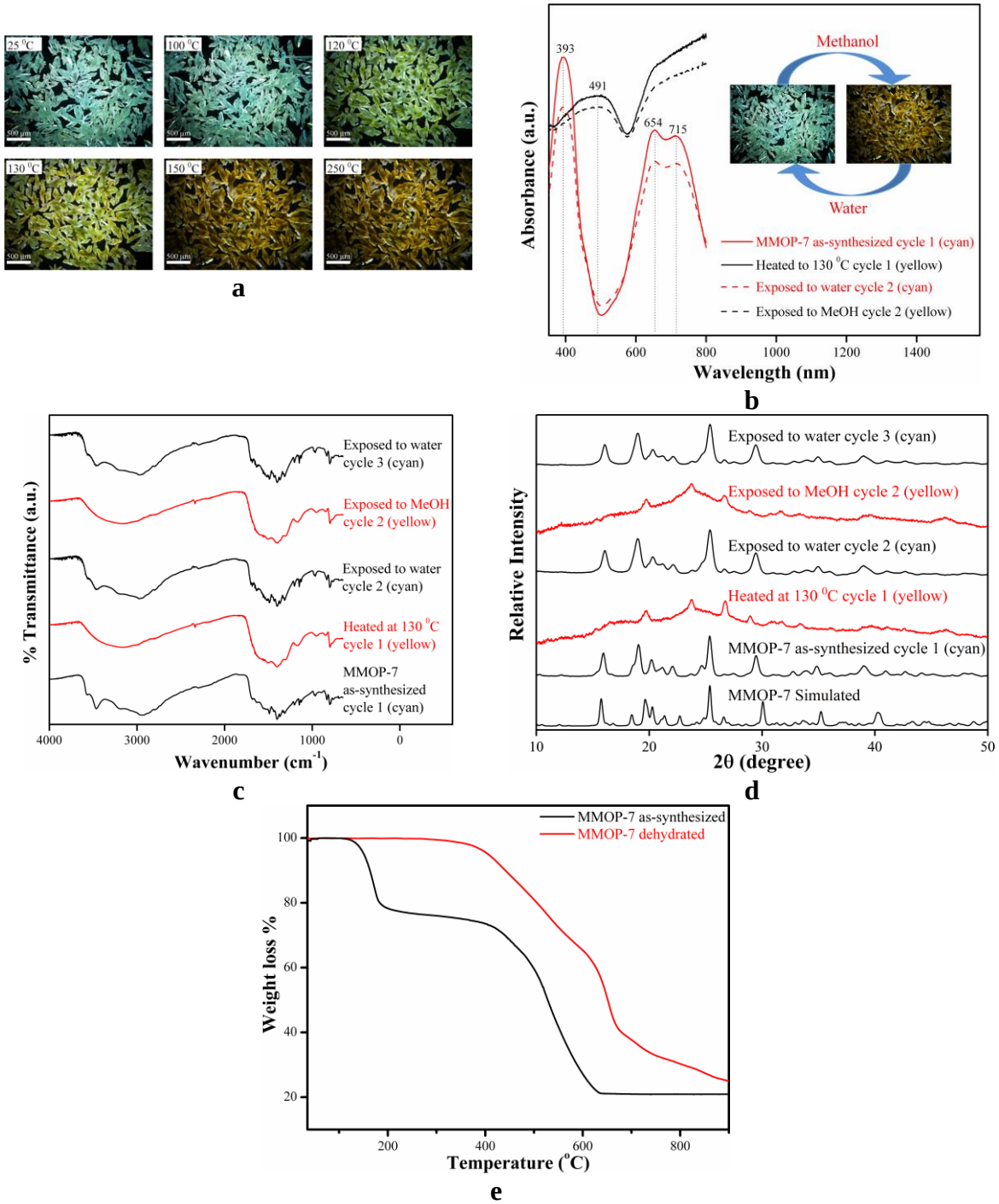

Figure S32. Chromic behaviour analysis of MMOP-**7** using. a) *In-situ* thermal microscopy images at different temperatures from 25-250 ºC (scale bar: 500 µm); b) UV-Vis spectra changes for MMOP-**7**. Black solid lines: MMOP-**7** as synthesized; purple solid lines: heated at 130 ºC, black dash lines: sample on exposure in water and red dash lines: sample on exposure in methanol. Insert: chromism images of MMOP-**7**; c) FTIR spectra of the MMOP-**7** as-synthesized, heated at 130 ºC, exposed to water and then exposed to methanol d) PXRD patterns of the samples taken at different cycles and the simulated patterns calculated from the single-crystal X-ray diffraction data. e) TG curves of MMOP-**7** as synthesized and dehydrated. One cycle is referred to a transformation that bring the cyan species to yellow species and return to the original colour.